Patient 3-Dimensional Reconstructed MRI Findings

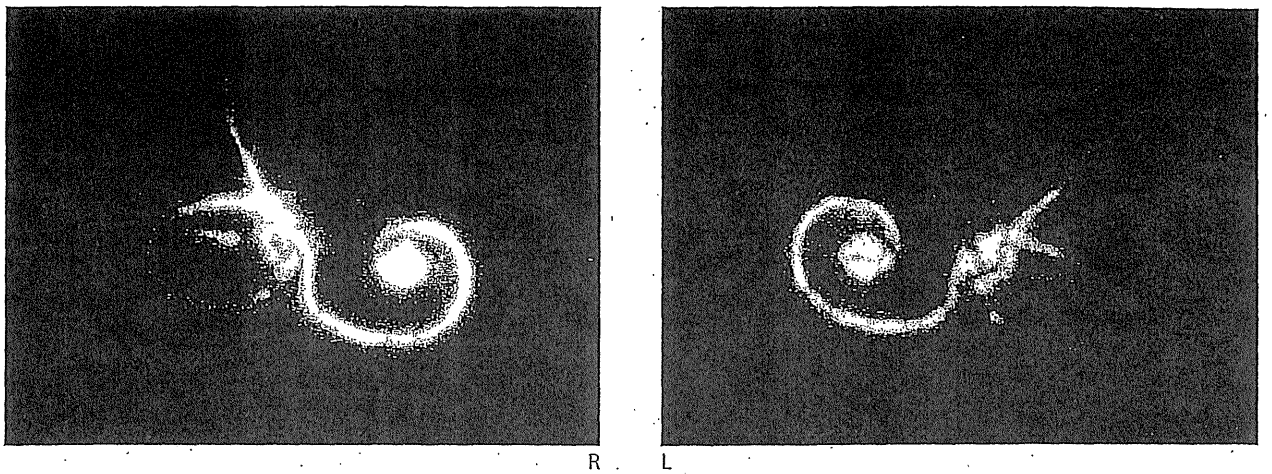

R L

Fig. 56. (Case 2) 3-dimensional reconstructed MRI

[Patient 3-Dimensional Reconstructed MRI Findings]
No clear abnormalities or bilateral differences exist in either the affected side (R) or the normal side (L).

Patient CT Findings

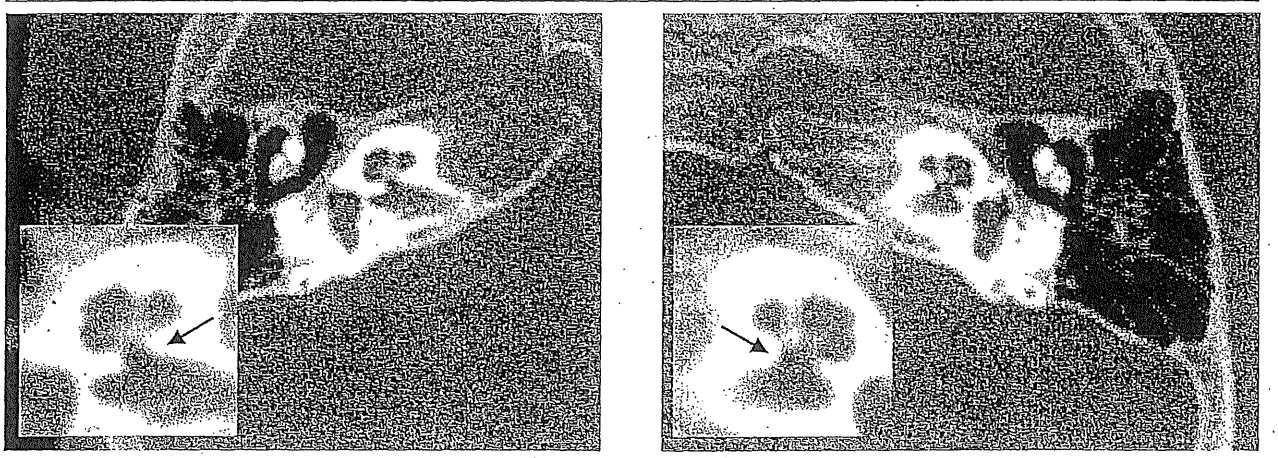

R. axial image L. axial image

Fig. 57. (Case 2) CT

[Patient CT Findings]
In the right ear, the diameter of the transitional area between the fundus of the internal auditory canal and the modiolus—the so-called cochlear nerve canal (covered later in more detail)— is 1.7 mm. This is clearly narrower (R: ↙, L: ↘) than the left ear, which is 2.4 mm. There are no other abnormal findings in the right inner or middle ear. In the left ear there are no abnormal findings whatsoever, including the fundus of the internal auditory canal.

Patient 3-Dimensional Reconstructed MRI Findings

In observing the inner ear in 3-dimensional reconstructed MR images, there were no clear abnormalities or bilateral differences (fig. 56).

Patient CT Findings

In the right ear, the diameter of the transitional area between the fundus of the internal auditory canal and the modiolus—the so-called cochlear nerve canal (covered later in more detail)— is 1.7 mm. This is clearly narrower than the left ear, which is 2.4 mm. There are no other abnormal findings in the right inner or middle ear. In the left ear there are no abnormal findings whatsoever, including the fundus of the internal auditory canal (fig. 57).

Patient MRI Findings

Observing the nerves at the fundi of the left and right internal auditory canals, the respective difference is evident, with the right cochlear nerve depicted indistinctly (fig. 58:1R) and the left cochlear nerve clearly visible (fig. 58:1L). The right internal auditory canal is also somewhat narrower, with a diameter of 2.4 mm compared to the left's 3.7 mm. Cranial nerve VIII itself is also thinner on the right (fig. 58:2R) than on the left (fig. 58:2L).

Patient MRI Findings

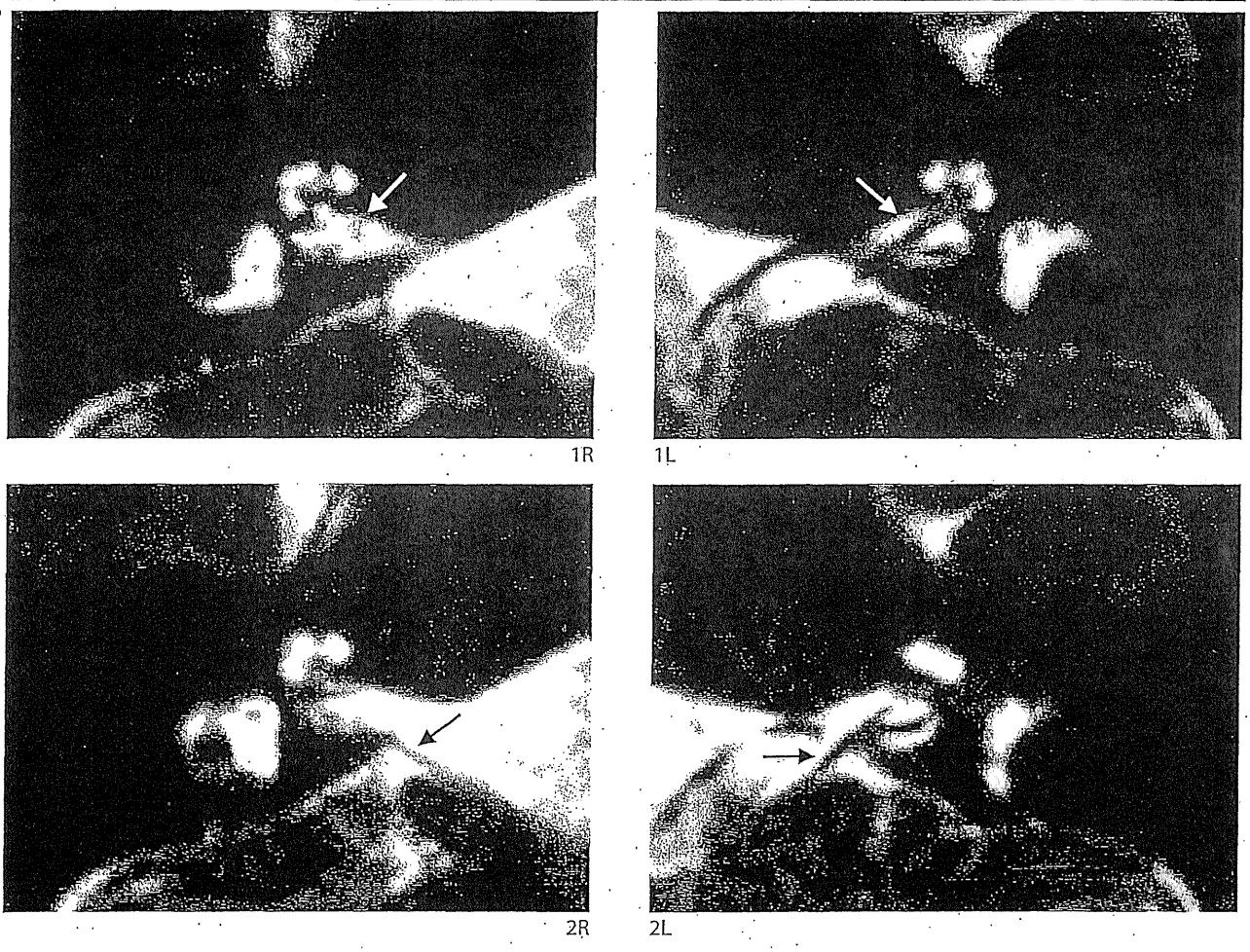

Fig. 58. (Case 2) MRI

[Patient MRI Findings]

Observing the nerves at the fundi of the left and right internal auditory canals, the respective difference is evident, with the right cochlear nerve depicted indistinctly (1R: ↙) and the left cochlear nerve clearly visible (1L: ↘). The right internal auditory canal is also somewhat narrower, with a diameter of 2.4 mm compared to the left's 3.7 mm. Cranial nerve VIII itself is also thinner on the right (2R: ↙) than on the left (2L: →).

Considerations and Diagnosis

In this case testing was conducted after the subject contracted meningitis and hearing loss was confirmed in the right ear, but as he was an infant and had not received newborn hearing screening, it was unclear as to whether or not the hearing loss existed prior to contracting meningitis. However, hearing loss due to bacterial meningitis normally arises through damage to both the sensory epithelium and the cochlear nerve due to inner ear infection and inflammation from the cochlear canaliculus or the internal auditory canal, so normal a DPOAE on the affected side, as is the case here, is exceptional. Also, ossification subsequent to labyrinthitis is thought to spread from the scala tympani or modiolus, at the basal turn of the cochlea where the cochlear canaliculus opens, to the cochlea and the entire inner ear, including the vestibule. It is very difficult to imagine that ossification would occur only in the cochlear nerve canal and make it narrower, as it has here. On the other hand, as we shall see later, there are many recent reports of congenital stenosis of the cochlear nerve canal at the fundus of the internal auditory canal, and this malformation is increasingly being recognized as a distinct disease entity. Based on the above considerations, we feel that this case, rather than being one of selective retrocochlear disturbance and ossification of the cochlear nerve canal caused by meningitis, is more likely one of retrocochlear hearing loss due to congenital hypoplasia of the cochlear nerve canal and cochlear nerve.

Cochlear Nerve Canal

The anteroinferior part of the internal auditory canal, referred to as the cochlear area, contains the tractus spiralis foraminosus through which the cochlear nerve bundles pass. While it forms a slight recess in the fundus of the internal auditory canal, no neural canal exists as a distinct anatomical structure. However, in some cases of sensorineural hearing loss, this area forms a narrow, tubular structure. As this tubular structure does not exist in normal anatomy and there is no official anatomical term for it, it was initially reported as the "bony canal for the cochlear nerve" [1], and later most often simply referred to as the "cochlear nerve canal" [2]. In cases of profound

hearing loss accompanied by cochlear nerve canal stenosis observed in CT images, hypoplasia of the cochlear nerve is often confirmed through MRI observations [3, 4]. Clinically, there is low expectation for the effectiveness of cochlear implants when cochlear nerve canal stenosis with cochlear nerve hypoplasia is present [3, 4], making it an important point to focus on during clinical imaging diagnosis for cases of congenital sensorineural hearing loss.

References

1 Fatterpekar GM, Mukherji SK, Alley J, et al: Hypoplasia of the bony canal for the cochlear nerve in patients with congenital sensorineural hearing loss: initial observations. Radiology 2000;215:243–246.

2 Stjernholm C, Muren C: Dimensions of the cochlear nerve canal: a radioanatomic investigation. Acta Otolaryngol 2002;122:43–48.

3 Miyasaka M, Nosaka S, Morimoto N, et al: CT and MR imaging for pediatric cochlear implantation: emphasis on the relationship between the cochlear nerve canal and the cochlear nerve. Pediatr Radiol 2010 Mar 23 [Epub ahead of print].

4 Papsin BC: Cochlear implantation in children with anomalous cochleovestibular anatomy. Laryngoscope 2005;115 (Suppl. 106):1–26.

Points

1. When the cause of sensorineural hearing loss is unclear, it is necessary to examine the cochlear nerve canal on the fundus of the internal auditory canal.
2. Cases of cochlear nerve canal stenosis are frequently accompanied by cochlear nerve hypoplasia.
3. Presence of cochlear nerve canal stenosis is an important factor when considering indication for cochlear implant surgery.

Case 3 IAC Malformation, Arachnoid Cyst of Fallopian Canal

Subject: male, 3 years old

History and Clinical Findings

Since around one year old the subject had experienced recurrent, bilateral acute otitis media along with repeated bouts of meningitis, and was referred to our department by a neighborhood otolaryngologist for testing to determine the cause of the meningitis. Another hospital had diagnosed right inner ear malformation and right-side deafness. Otitis media was recurring bilaterally, and our findings at time of initial exam indicated retraction of the tympanic membranes in both ears, along with effusion accumulation in the right ear. Hearing testing showed right-side deafness, with a hearing level of 30–40 dB in the left ear. Temporal bone CT and MRI exams were carried out.

Patient CT Findings

Mastoid air cell development is deficient on both sides and a soft tissue density (effusion) can be seen between the epitympanum and the mastoid segment, but no abnormalities can be ascertained in the ossicles. In the right inner ear, a portion of the basal turn of the cochlea, the vestibule, and the ampulla of the posterior semicircular canal are discernible, but other parts are ossified (fig. 59:1R, 2R, 3R). There is no clear stenosis or enlargement of the internal auditory canal, but starting at the fundus of the internal auditory canal the labyrinthine segment of the right facial nerve (fig. 59:3R) is enlarged compared to the normal control (fig. 59:n3), and in the part normally corresponding to the area between the geniculate ganglion and the tympanic segment of the facial nerve (fig. 59:n2), a soft tissue density of around 6.2 × 2.4 mm, longer anteroposteriorly, (fig. 59:2R, 3R) is visible. This continues posteriorly to become the tympanic and mastoid segments of the facial nerve, with no abnormalities in the peripheral fallopian canal.

Observing the coronal CT image, a thick neural canal can be identified running from the internal auditory canal directly to the geniculate ganglion (fig. 60:3R). Anterior to this, whereas in the normal control the area around and superior to the geniculate ganglion (fig. 60:n1) is composed of air cells, in this case it is occupied by a large, saccular structure with a superoinferior diameter of over 5 mm (fig. 60:1R, 2R). Please refer to the normal control images to confirm the proper path of the facial nerve's labyrinthine segment (fig. 60:n2, n3) and tympanic segment (fig. 60:n2, n3).

Patient MRI Findings

When observed in the MRI, it is apparent that the facial nerve (fig. 61:1R) actually passes inside the facial nerve labyrinthine segment on the fundus of the internal auditory canal that was observed in the CT images. The cystic area of the geniculate ganglion is hyperintense (fig. 61:1R, 2R) in T2 weighted imaging and is continuous with the internal auditory canal and may be filled with cerebrospinal fluid. Also, inside this area there is a slightly hypointense structure (fig. 61:2R) that is assumed to be either

Patient CT Findings

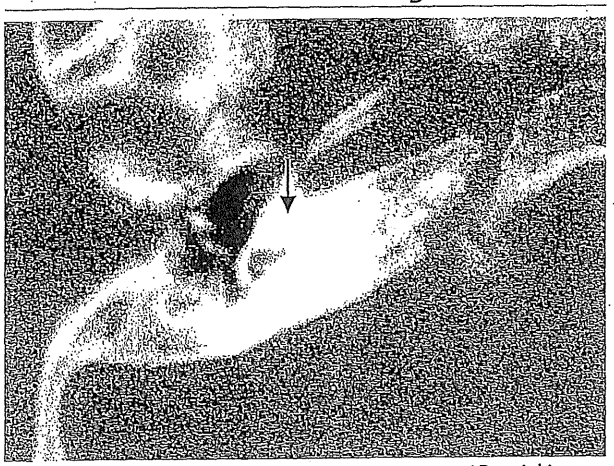

1R. axial image

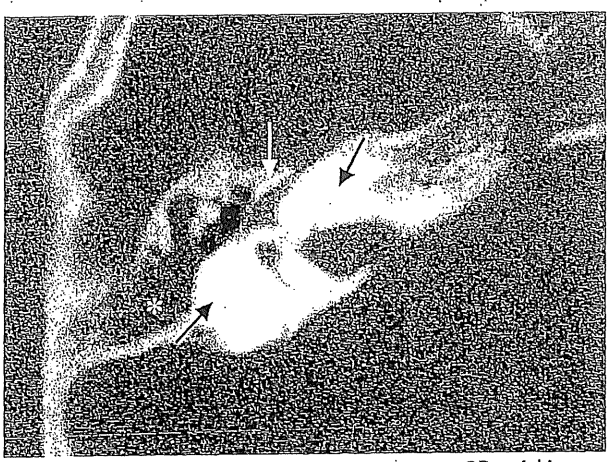

2R. axial image

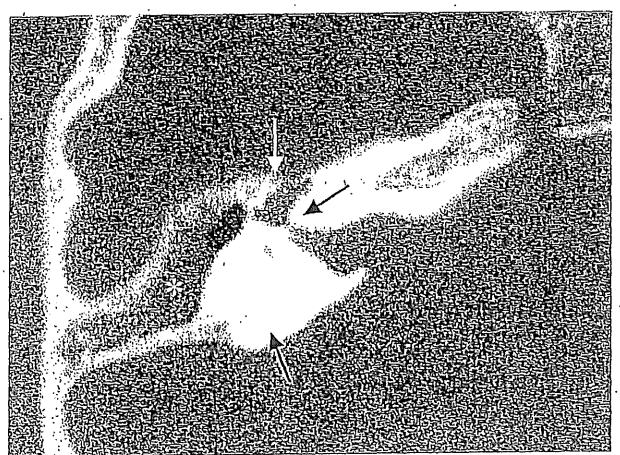

3R. axial image

Normal Control CT Findings

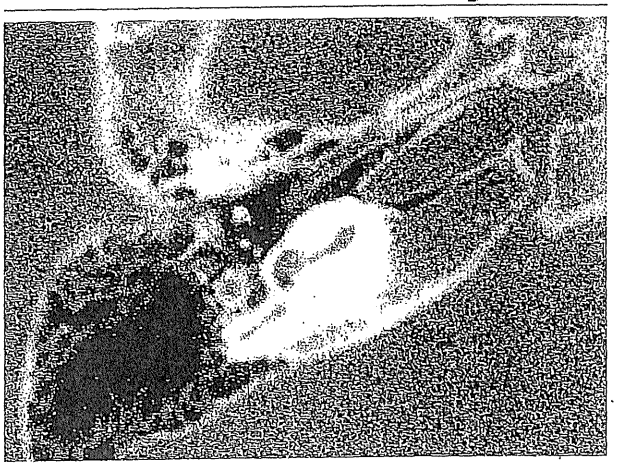

n1. axial image

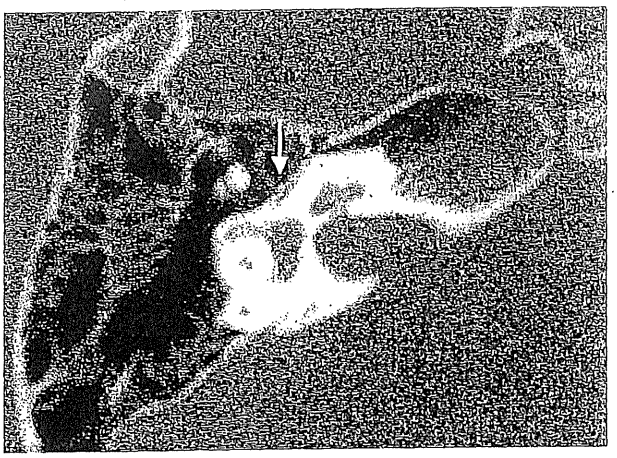

n2. axial image

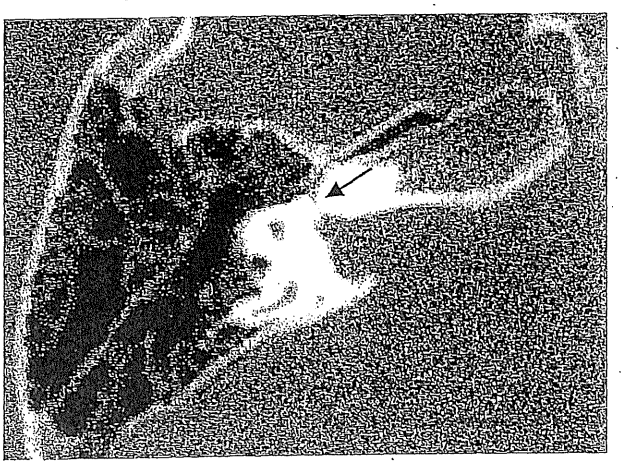

n3. axial image

Fig. 59. (Case 3) CT

[Patient CT Findings]

Mastoid air cell development is deficient and a soft tissue density (effusion) can be seen between the epitympanum and the mastoid segment, but no abnormalities can be ascertained in the ossicles. In the right inner ear, a portion of the basal turn of the cochlea, the vestibule, and the ampulla of the posterior semicircular canal are discernible, but other parts are ossified (1R ↓, 2R ↙ ↗, 3R ↖). There is no clear stenosis or enlargement of the internal auditory canal, but starting at the fundus of the internal auditory canal the labyrinthine segment of the right facial nerve (3R: ↙) is enlarged, and in the part normally corresponding to the area between the geniculate ganglion and the tympanic segment of the facial nerve, a soft tissue density of around 6.2 × 2.4 mm, longer anteroposteriorly, (2R: ⇩, 3R: ⇩) is visible. No abnormalities were found in the peripheral fallopian canal.

《Normal Control CT Findings》

n1: cross-section enabling examination of the basal turn of the cochlea. n2: ⇩ tympanic segment of the facial nerve. n3: ↙ labyrinthine segment of the facial nerve.

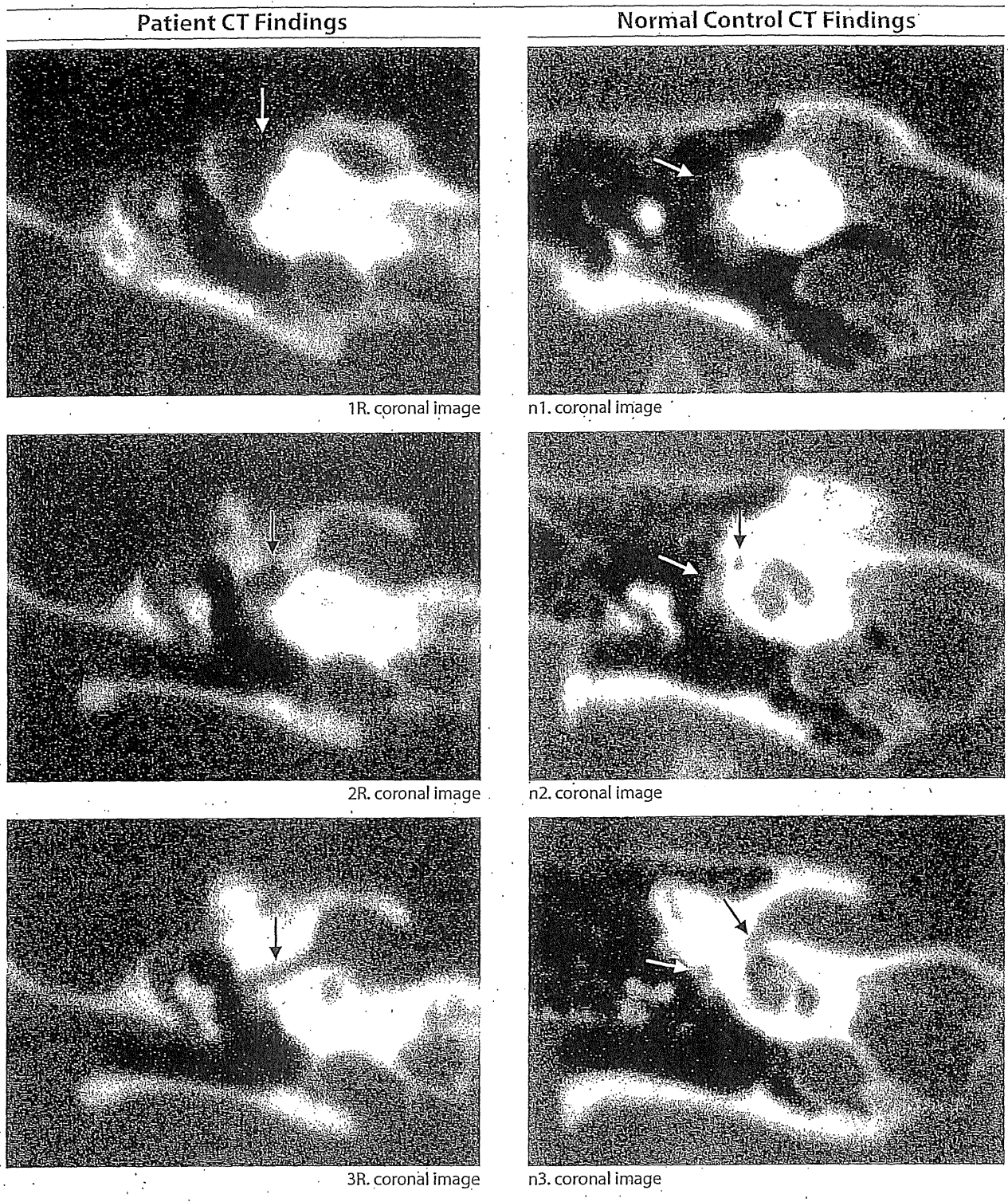

Fig. 60. (Case 3) CT

[Patient CT Findings]

A thick neural canal can be identified running from the internal auditory canal directly to the geniculate ganglion (3R: ↓). Anterior to this, a large, saccular structure can be observed (1R: ⇩, 2R: ↓). Please refer to the normal control images to confirm the proper path of the facial nerve's labyrinthine segment (n2: ↓, n3: ↘) and tympanic segment (n2: ↝, n3: ↝).

《Normal Control CT Findings》

n1: ↝ geniculate ganglion. n2: ↓ labyrinthine segment of facial nerve; ↝ tympanic segment of facial nerve. n3: ↘ labyrinthine segment of facial nerve; ↝ tympanic segment of facial nerve.

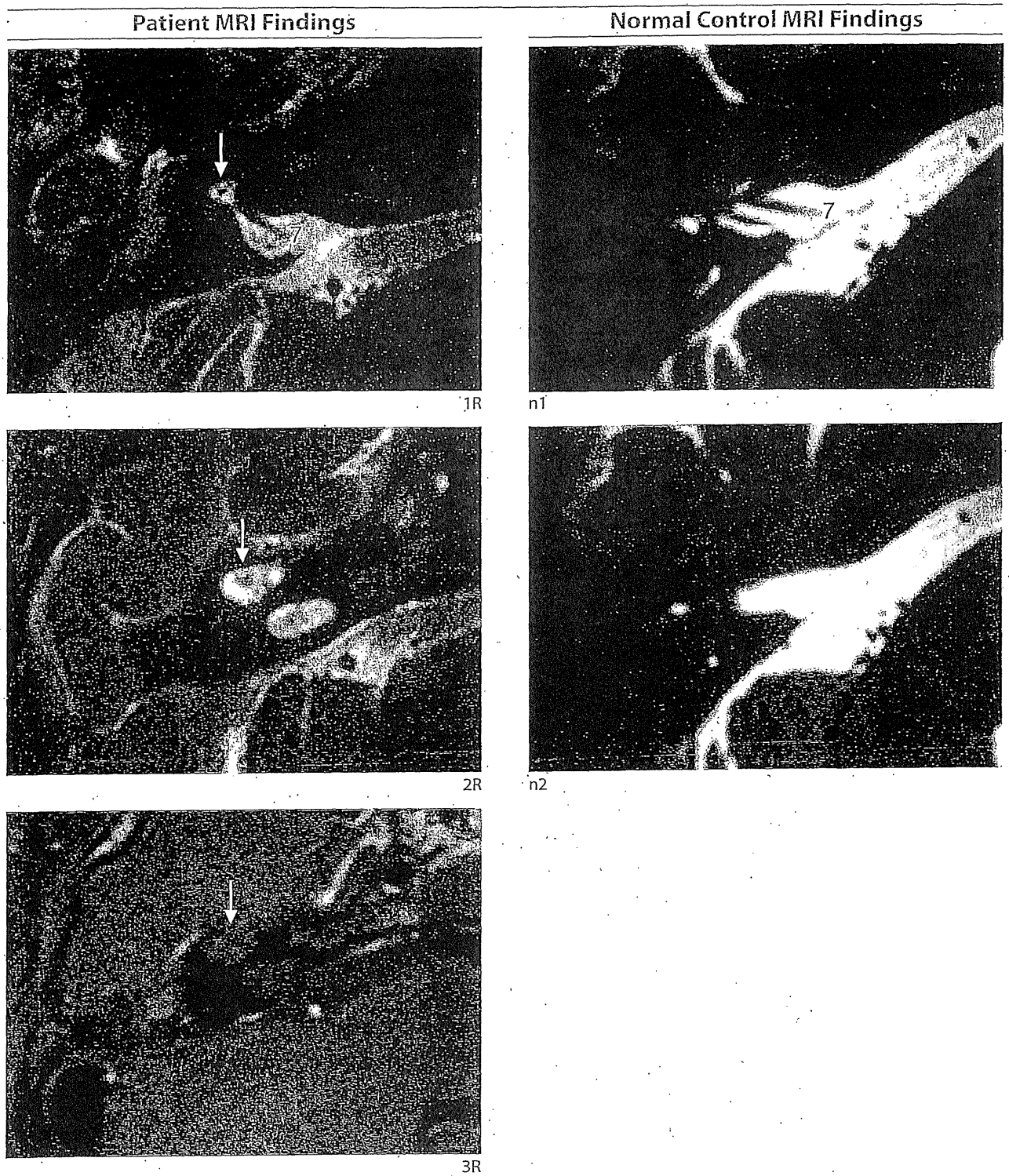

Fig. 61. (Case 3) MRI

[Patient MRI Findings]

It is apparent that the facial nerve (1R: 7) actually passes inside the facial nerve labyrinthine segment on the fundus of the internal auditory canal. The cystic area of the geniculate ganglion is hyperintense (1R & 2R:) in T2 weighted imaging and is continuous with the internal auditory canal and may be filled with cerebrospinal fluid. Also, inside this area there is a slightly hypointense structure (2R:) that is assumed to be either nerve fibre or some kind of soft tissue. In T1 weighted Gd enhanced MRI performed later, neither the interior nor the margins of this cystic structure revealed contrast enhancement (3R:), contraindicating a tumor, granulation, cholesteatoma, or other lesion.

《Normal Control MRI Findings》

n1: 7 indicates the facial nerve inside the internal auditory canal. n2: In a hyperintense T2 weighted image such as this, the geniculate ganglion located lateroanterior to the fundus of the internal auditory canal is barely discernible.

nerve fibre or some kind of soft tissue. In T1 weighted Gd enhanced MRI performed later, neither the interior nor the margins of this cystic structure exhibited contrast enhancement (fig. 61:3), contraindicating a tumor, granulation, cholesteatoma, or other lesion.

Also, on close inspection of the simple T2 weighted cranial MRI (fig. 62), there is a T2 hyperintense area extending from the area posterior to the right ear subcutaneously below the ear, which may be accumulation of cerebrospinal fluid leaked from the fallopian canal.

Clinical Course and Surgical Findings

Initially, based on the CT findings in this case, I assumed that the bony defect in the geniculate ganglion area was either a cyst or a congenital cholesteatoma, but in the MRI there was no contrast enhancement around the margin and it was continuous with the internal auditory canal, so I concluded there was a high probability that it was an arachnoid cyst that had herniated and enlarged into the fallopian canal. I hypothesized that this had led to effusion of cerebrospinal fluid into the fallopian canal, with retrograde infection from the area communicating with the middle ear, which gave rise to recurrent meningitis. Later the subject again contracted severe meningitis, which caused paresis of the right facial nerve around one year after our initial consultation, so we inspected the geniculate ganglion using a temporal craniotomy/middle cranial fossa approach with the objective of arresting the cerebrospinal fluid leak by opening, confirming, and obliterating the lesion site. As suggested from the MR images, the area consisted of a cyst covered in a thin membrane, the incision of which resulted in a strong outflow of spinal fluid. Inside was a cobweb-like fibrous structure, possibly the facial nerve. The area where the cyst flowed in from the fundus of the internal auditory canal was patched with several layers of periosteum fragments and glued in place. The inside of the cyst was also filled with bone putty, but in order to avoid permanent facial paralysis we were careful not to pack the space too firmly.

Postoperatively the facial paralysis worsened slightly, but there was no recurrence of the meningitis. Middle ear ventilation tube insertion and other therapies to prevent recurrence of middle ear infection were also pursued concurrently. However, one year later there was a reoccurrence of severe meningitis, so after consultation with the parents it was decided to completely obliterate and close the cyst area, even though it may not be possible to preserve facial nerve function.

Two years six months after initial examination in our department, a right temporal craniotomy was once again performed and the cyst in the geniculate ganglion opened up via the middle cranial fossa. This time the area was opened broadly all the way to the internal auditory canal and the labyrinthine segment of the fallopian canal packed firmly with periosteum fragments. The interior of the cyst was filled with bone putty that was strongly compacted without regard for facial nerve damage. Histopathological examination of the specimen collected at this time confirmed that the wall of the cyst was arachnoid membrane. Postoperatively, the facial nerve score fell temporarily, but then gradually recovered, and currently has improved to partial paresis. Also, there has been no recurrence of meningitis up to this time, two years six months after revision surgery.

Patient MRI Findings

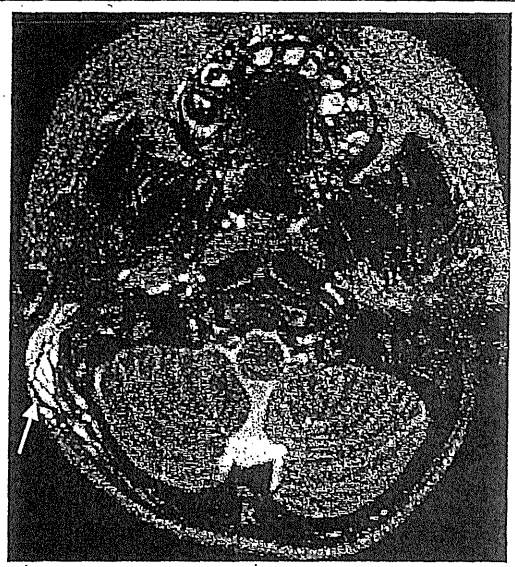

T2 weighted image

Fig. 62. (Case 3) MRI.

[Patient MRI Findings]

There is a T2 hyperintense area extending from the area posterior to the right ear subcutaneously below the ear (↑), which may be accumulation of cerebrospinal fluid leaked via the fallopian canal.

Arachnoid Cyst of Fallopian Canal

It is common to observe the arachnoid membrane forming a cyst and enlarging intracranially, but these cysts are often asymptomatic and require no particular treatment. However, on rare occasions the arachnoid cyst may herniate outside the cranium and present a variety of pathological findings, including meningitis. In particular, there are cases of cysts developing peripherally within the fallopian canal of the temporal bone along the path of the facial nerve, with recurring meningitis. Aside from this case, we have also experienced a similar case in an adult.

There have been several reports to date concerning cases of cerebrospinal fluid leak via along the fallopian canal due to congenital defects, in which retrograde infection caused recurring meningitis [1–3]. The area surrounding the geniculate ganglion is one route along which cholesteatomas develop from the epitympanum to the petrous apex, and in a differential diagnosis cholesteatoma is

what first comes to mind. In this case, however, the MRI signal characteristics differed from that of a cholesteatoma, and the finding of cerebrospinal fluid emanating subcutaneously from the stylomastoid foramen would not occur with cholesteatoma, so knowledge of this disease facilitates correct diagnosis. In our surgical findings, the nerve inside the cyst did not form a simple bundle as usual, but instead, except for the main nerve bundle, spread out like a cobweb of fine fibers. The poorly defined hypointense area observed inside the cyst in the T2 weighted MRI is how the separated nerve bundles or fibers within the cyst are depicted.

Concerning treatment, in all previously reported cases it has been difficult to find a balance between the need to completely block cerebrospinal fluid leak and concern for damage to the facial nerve as a result of surgery, as failure to firmly block the fallopian canal will result in recurrence of meningitis. In this case also, the area around the facial nerve was initially sealed lightly to avoid nerve damage, but due to the later recurrence of possibly life-threatening meningitis, in the second operation the parents were fully consulted and the cyst cavity firmly obliterated without regard to preservation of facial nerve function, finally preventing the meningitis from reoccurring. However, because we avoided removing the facial nerve before obliterating the cavity, there has been considerable long-term recovery of facial nerve function. A trans-mastoid approach has been attempted for a case of cerebrospinal fluid leakage and meningitis similar to this one [2], but control of leakage was difficult and in the end required subtotal extirpation of the temporal bone. Approaching via the middle cranial fossa is comparatively minimally invasive and effective and should be considered one of the surgical options in treatment of cerebrospinal fluid leak via the fallopian canal.

Points

1. The fallopian canal is sometimes the causative route for infant meningitis.
2. Herniation of an arachnoid cyst through the fallopian canal can cause facial paralysis, cerebrospinal fluid leak, and meningitis.
3. Obliteration of the region of the geniculate ganglion and labyrinthine segment of the facial nerve via the middle cranial fossa was an effective treatment.

References

1 Foyt D, Brackmann DE: Cerebrospinal fluid otorrhea through a congenitally patent fallopian canal. Arch Otolaryngol 2000;126:540–542.

2 Isaacson JE, Linder TE, Fisch U: Arachnoid cyst of the fallopian canal: a surgical challenge. Otol Neurotol 2002;23:589–593.

3 Mong S, Goldberg AN, Lustig LR: Fallopian canal meningocele: report of two cases. Otol Neurotol 2009;30:525–528.

Author

Yasushi Naito, M.D.

1980 Resident, Dept. of Otolaryngology, Kyoto University Hospital
1981 Staff, Dept. of Otolaryngology, Kyoto National Hospital
1990 Visiting Scholar, UCLA School of Medicine, Prof. Vicente Honrubia
1992 Lecturer, Dept. of Otolaryngology, Kyoto University School of Medicine
2004 Director of Otolaryngology, Kobe City Medical Center General Hospital
Clinical Professor of Otolaryngology-Head and Neck Surgery, Kyoto University
2009 Vice President for Research and Education,
Kobe City Medical Center General Hospital

Memberships:
Oto-Rhino-Laryngological Society of Japan (Councilor)
Japan Otological Society (Councilor)
Japan Audiological Society (Board Member)
Japan Society for Equilibrium Research (Board Member)
Association for Research in Otolaryngology (USA)
Collegium Oto-Rhino-Laryngologicum Amicitiae Sacrum (CORLAS)
Barany Society

Acknowledgments

The Japanese edition of this book was published in April 2011. A section on incomplete partition type III anomaly of the inner ear was added for the current English edition. Some clinical studies in this book were supported by Grants-in-Aid for Scientific Research (C) 22591894 from the Japan Ministry of Education, Science and Culture.

I acknowledge with gratitude the contribution of Dr. Levent Sennaroglu, Professor of Otolaryngology, Hacettepe University, Turkey, not only for writing a special article on IP-III for this book, but also for his epoch-making scientific achievement in the classification of inner ear anomalies, which greatly helped in making the description of inner ear anomalies in this book more lucid and systematic.

I am indebted to Dr. Iwao Honjo, Professor Emeritus of Kyoto University, for supervising the first edition of the Japanese version of this book, and Dr. Kimitaka Kaga, Professor Emeritus of Tokyo University, for his warm support concerning the publication of this book. I offer my sincere gratitude to Mr. Atsushi Moriyama, of International Medical Publishers Ltd., who realized the publication of both the Japanese and English editions of this book, and Mr. Peter Roth, of Karger Medical and Scientific Publishers, for helping us to create the English edition. I thank Drs. Kyo Ito and Sho Koyasu, Department of Radiology, Kobe City Medical Center General Hospital, for their great help in clinical imaging, the members of Hyogo Otolaryngologist Society for introducing important patients who appear in this book, and the editorial staff of International Medical Publishers Ltd., for their professionalism in editing this book. I am grateful to Dr. Toru Kita, President of Kobe City Medical Center General Hospital, Dr. Haruhiko Kikuchi, Board Chairman of Kobe City Hospital Organization, and Dr. Juichi Ito, Professor of Otolaryngology-Head and Neck Surgery, Kyoto University, for their continuous support and supervision on clinical works and research in the hospital.

Finally, I want to thank my colleagues in our department: Drs. Shogo Shinohara, Yosaku Shiomi, Keizo Fujiwara, Masahiro Kikuchi, Hiroshi Yamazaki, Yuji Kanazawa, Risa Kurihara, Ippei Kishimoto, Hiroyuki Harada, Satoshi Kakutani, Tsunemichi Adachi, Shin-ya Hori, Yosuke Tona; speech therapists Saburo Moroto, Tomoko Yamazaki, and Rinko Yamamoto; and department secretary Noriyo Sakamoto.

Gene Therapy (2012) 19, 1141–1149

www.nature.com/gt

ORIGINAL ARTICLE

Topical application of the antiapoptotic TAT-FNK protein prevents aminoglycoside-induced ototoxicity

A Kashio[1], T Sakamoto[1], A Kakigi[1], M Suzuki[2], K Suzukawa[1], K Kondo[1], Y Sato[3], S Asoh[3], S Ohta[3] and T Yamasoba[1]

We previously demonstrated that an artificial protein, TAT-FNK, has antiapoptotic effects against cochlear hair cell (HC) damage caused by ototoxic agents when applied systemically. To examine the feasibility of topical protein therapy for inner ear disorders, we investigated whether gelatin sponge soaked with TAT-FNK and placed on the guinea pig round window membrane (RWM) could deliver the protein to the cochlea and attenuate aminoglycoside (AG)-induced cochlear damage *in vivo*. First, we found that the immunoreactivity of TAT-myc-FNK was distributed throughout the cochlea. The immunoreactivity was observed from 1–24 h after application. When Tat-FNK was applied 1 h before ototoxic insult (a combination of kanamycin sulfate and ethacrynic acid), auditory brainstem response threshold shifts and the extent of HC death were significantly attenuated. When cochlear organotypic cultures prepared from P5 rats were treated with kanamycin, TAT-FNK significantly reduced the extent of caspase-9 activation and HC death. These findings indicate that TAT-FNK topically applied on the RWM can enter the cochlea by diffusion and effectively prevent AG-induced apoptosis of cochlear HCs by suppressing the mitochondrial caspase-9 pathway.

Gene Therapy (2012) **19,** 1141–1149; doi:10.1038/gt.2011.204; published online 22 December 2011

Keywords: protein therapy; apoptosis; cochlea; aminoglycoside; topical application

INTRODUCTION

Apoptosis is involved in cochlear sensory hair cell (HC) death caused by a variety of insults, which include acoustic trauma, loss of trophic factor support, ischemia–reperfusion, and exposure to ototoxic agents such as aminoglycoside (AG) antibiotics and the anti-neoplastic agent cisplatin.[1–3] Protecting cells from apoptosis by controlling the balance of pro- and antiapoptotic proteins by techniques such as gene therapy is considered a good strategy for protection of HCs from ototoxic insults. Overexpression of Bcl-2 proteins by delivery of the *Bcl-2* gene into HCs has been reported to prevent the degeneration of HCs exposed to AG or cisplatin.[4] Injection of the *Bcl-x_L* gene into mice cochlea also prevents HC degeneration induced by kanamycin.[5] However, such gene transfer application cannot control the amount or exposure time of the target protein to achieve optimal prevention of cell death. In addition, gene transfer technology cannot avoid the possibility of detrimental insertion of transgenes. Therefore, injection of the target protein could be an alternative method. For example, several proteins such as granulocyte-colony stimulating factor[6] have already been used in clinics. Such protein therapy, however, is not always applicable for treatment of inner ear disorders because the blood–labyrinth barrier may inhibit the delivery of high-molecular-weight proteins into the cochlea. This problem may be solved by using the protein transduction domain technology. When fused with a protein transduction domain such as the TAT domain of the HIV/Tat (transcription-transactivating) protein, a variety of high-molecular-weight proteins have been successfully introduced into cells both *in vitro* and *in vivo*.[7,8]

We first constructed a powerful artificial antiapoptotic protein, FNK (originally designated Bcl-xFNK by Asoh *et al.*[9]), which has three amino-acid substitutions, Tyr-22 to Phe(F), Gln-26 to Asn(N) and Arg-165 to Lys(K), to strengthen the cytoprotective activity of Bcl-x_L. We then demonstrated that fusion of FNK with TAT enabled FNK to penetrate highly negatively charged chondrocytes[9,10] and the blood–brain barrier,[11] and that TAT-FNK showed an antiapoptotic effect in a model of brain and hepatic ischemia.[11,12] When injected intraperitoneally into guinea pigs *in vivo*, we observed that TAT-FNK was distributed widely in the cochlea and that it reduced the expression of cleaved poly-(ADP-ribose)-polymerase (PARP), auditory brainstem response (ABR) threshold shifts, and HC loss induced by a combination of ethacrynic acid (EA) and kanamycin sulfate (KM), *in vivo*.[13]

Another potential drug delivery system for treatment of cochlear disorders is topical drug application into the middle ear space. Compared with systemic injections, such local delivery is beneficial because it requires significantly lower amounts of drug and reduces systemic side effects. A major side effect after long-term administration of an antiapoptotic drug is a possibility of carcinogenesis. Overexpression of Bcl-x_L, the original protein of FNK, is reported to have the potential to cause tetraploidization, which would result in neoplasia.[14,15] Schuknecht[16] has developed a topical drug application technique for inner ear disorders: injection of streptomycin into the middle ear space of patients with Ménière's disease. Intra-tympanic dexamethasone injections have also been performed as primary treatment for sudden sensorineural hearing loss.[17] Intra-tympanic drug application has also been used in animal studies to examine the effects on inner ear function or disorders. It is quite difficult, however, to achieve the delivery of high-molecular-weight proteins into the inner ear because these proteins cannot pass through the round window membrane (RWM), which is the main route into the inner ear.

[1]Faculty of Medicine, Department of Otolaryngology and Head and Neck Surgery, The University of Tokyo, Tokyo, Japan; [2]Department of Otolaryngology and Head and Neck Surgery, Sakura Medical Center, Toho University, Chiba, Japan and [3]Department of Biochemistry and Cell Biology, Institute of Development and Aging Sciences, Graduate School of Medicine, Nippon Medical School, Kanagawa, Japan. Correspondence: Professor T Yamasoba, Department of Otolaryngology and Head and Neck Surgery, The University of Tokyo, Hongo 7-3-1, Bunkyo-ku, Tokyo 113-8655, Japan.
E-mail: tyamasoba-tky@umin.ac.jp
Received 13 May 2011; revised 9 November 2011; accepted 14 November 2011; published online 22 December 2011

In the current study, we examined whether the TAT fusion technique could make transtympanic protein therapy applicable for inner ear disorders. We investigated whether TAT-FNK applied topically on the RWM could be successfully delivered into the cochlea, and protect cochlear HCs from an ototoxic combination of KM and EA. We also investigated whether TAT-FNK could prevent HC death caused by KM by suppression of the mitochondrial caspase-9 pathway.

RESULTS

Transduction of TAT-myc-FNK into cochlear tissue

Immunohistochemical staining using an anti-myc-tag antibody revealed that TAT-myc-FNK was detectable in the cochlea from 1 to 24 h after the application onto the RWM. There was a statistically significant difference between the groups as determined by one-way analysis of variance (ANOVA) ($F_{6,203}=41.239$, $P<0.01$). Scheffe's *post hoc* test revealed that the labeling indices (LIs) at 1, 3, 6, 12 and 24 h were significantly higher than that of the control ($P<0.01$). The LIs gradually increased from 1 to 6 h, but no differences were observed among the LIs at 1, 3 and 6 h. Beginning 12 h after the application, the LIs gradually decreased. The LIs at 6 and 12 h, 6 and 24 h, and 3 and 24 h were significantly different ($P<0.01$). No significant difference was observed between the LI of the control and that at 48 h (2a). High-power views of the organ of Corti (OC) and the spiral ganglion revealed that many spots consisting of TAT-myc-FNK were localized within the cells outside their nuclei (Figures 1b and c). The basal turn tended to show higher immunoreactivity than the upper turns, but there was no statistically significant difference between the cochlear turns at 1 and 6 h. Two-way ANOVA was conducted to examine the cochlear turns and the time course. There were no interactions between the two factors ($F_{2,174}=0.051$, $P=0.950$). There was also no statistical difference in the main effect of the cochlear turns ($F_{2,174}=1.033$, $P=0.358$; Figure 2b). In addition to the OC, the spiral ganglion cells (SGCs), the stria vascularis (SV) and spiral ligament (SL) also appeared to show greater immunoreactivity than the control 6 h after the application of TAT-myc-FNK onto the RWM. Because the background immunoreactivity in the control sections varied between the organs, the normalized LIs, that is, the ratio of the LIs in each organ to those of the control, of these organs were compared by one-way ANOVA. There was a statistically significant difference between the groups ($F_{3,116}=39.257$, $P<0.01$). Scheffe's *post hoc* test revealed that immunoreactivity was strongest in the cells in the OC, followed by that in the SGCs. The normalized LI of the OC was significantly greater than that of the SGCs, the SV and the SL ($P<0.01$). The normalized LI of the SGCs was also significantly higher than that of the SV and the SL ($P<0.01$; Figure 2c). Specific immunoreactivity to myc was not observed in any control ears that were administered only myc-FNK (that is, without TAT) or in the ears of animals administered TAT-myc-FNK in the contralateral ear (Figure 1d).

Protective effects of TAT-FNK against ABR threshold shifts induced by ototoxic insults

The baseline ABR thresholds measured before ototoxic insult were statistically not different at all tested frequencies among animals (data not shown). Neither experimental nor drug control animals showed any signs of systemic illness, such as diarrhea or hair loss, until euthanasia. For drug control animals, a gelatin sponge soaked with TAT-FNK was placed on the RWM, but a combination of KM and EA was not given. These animals showed no ABR threshold shifts at any tested frequency (data not shown), indicating that topical application of TAT-FNK on the RWM is not harmful to cochlear function.

ABR threshold shifts 14 days after the ototoxic insult in the experimental animals are shown in Figure 3 ($n=8$ each). Two-way ANOVA was conducted to examine the effect of the TAT-FNK administration and the frequency on the ABR threshold shifts. There was no significant interaction between TAT-FNK administration and hearing frequency ($F_{2,42}=0.042$, $P=0.959$). There was a main effect of TAT-FNK administration ($F_{1,42}=27.355$, $P<0.01$) but no significant difference in frequency ($F_{2,42}=0.833$, $P=442$),

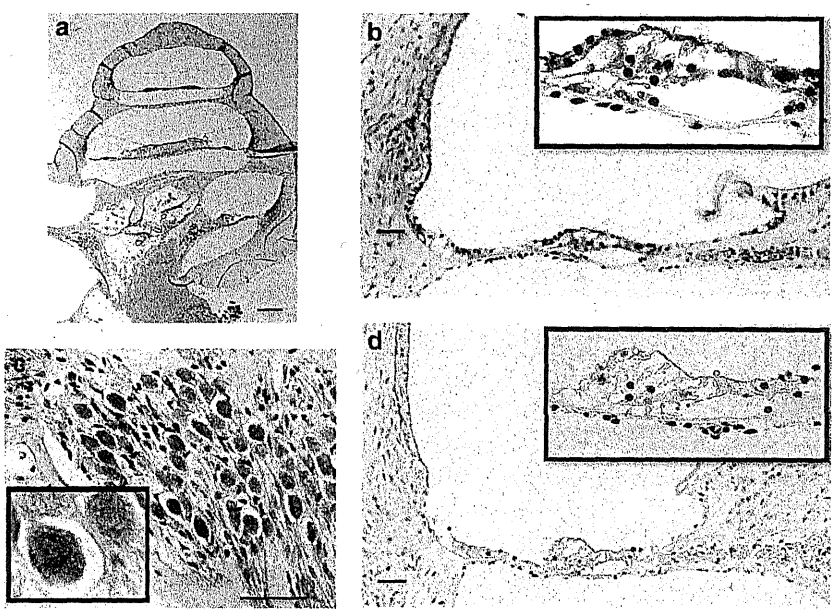

Figure 1. Transduction of TAT-myc-FNK protein into guinea pig cochlea. (**a**–**c**) The anti-myc-tag antibody was used to stain TAT-myc-FNK. Entire cochlea (**a**). An enlarged image of the OC (**b**) and the spiral ganglion (**c**). The insets in panels **b** and **c** are high-power views of the cells in the OC and SGCs, respectively. (**d**) An image of the contralateral ear, with a high-power view of OC in the insets. Scale bar: 200 μm, panel **a**; 40 μm, **b**–**d**.

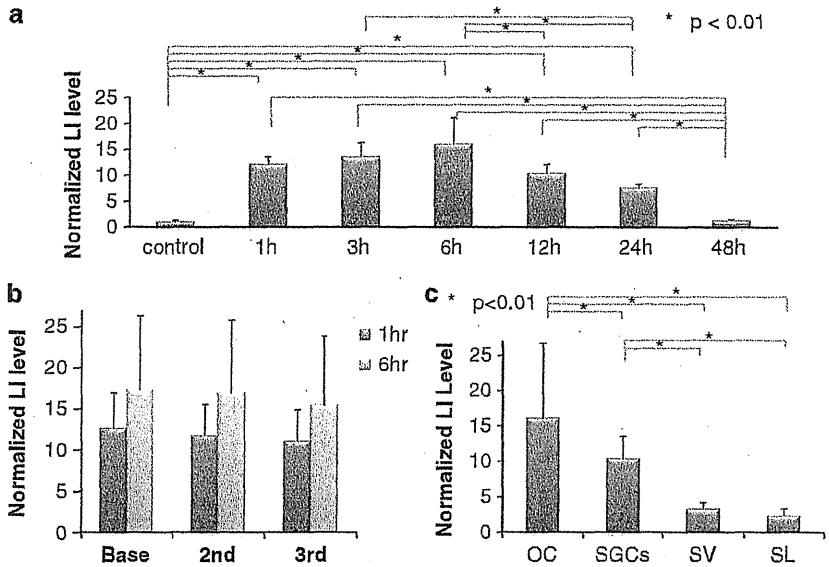

Figure 2. LIs for TAT-myc-FNK immunostaining of the inner ear. The time course of the normalized LIs level for immunostaining of the OC is shown (**a**). Error bar: s.d. $*P<0.01$. (**b**) Normalized LIs for each turns at 1 and 6 h after application of TAT-myc-TNK. (**c**) Normalized LIs at 6 h for OC, SGCs, the SV and the SL. Error bar: mean (s.d.). $*P<0.01$.

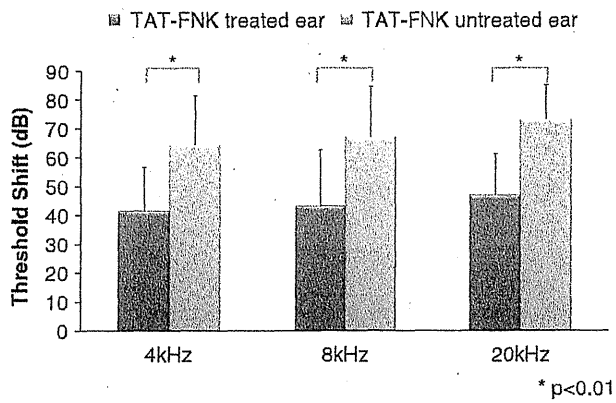

Figure 3. ABR threshold shifts at each tested frequency in both TAT-FNK treated and untreated ears. Pure tone 4, 8 and 20-kHz ABR threshold shifts before ototoxic insult and 14 days after the insult are shown. The dark gray bars indicate the values for the TAT-FNK-treated ears. The light gray bars indicate the values for the TAT-FNK-untreated ears. Error bar: s.d. $*P<0.01$.

indicating that the ABR threshold shifts were significantly smaller at all the tested frequencies in the TAT-FNK-treated ears than in the untreated contralateral ears. This result suggests that the TAT-FNK treatment significantly attenuated the ABR threshold shifts induced by the ototoxic agents.

HC protective effects of TAT-FNK *in vivo*

Figures 4a and b show the average cytocochleograms in the TAT-FNK-treated and contralateral untreated ears, respectively, which were produced by plotting the average percentage of HC loss in every segment between 5 and 16 mm from the apex that was averaged across all subjects ($n=6$ each). Segments measuring under 5 mm and over 16 mm were excluded because the extent of HC damage could not be quantified owing to damage in some samples during surface preparation. The frequency map was added in the *x*-axis according to the data of Tsuji and Liberman.[18]

The ototoxic agents induced losses of 91.7 ± 7.0% of the outer HCs (OHCs) and 13.8 ± 5.9% of the inner HCs (IHCs) in the TAT-FNK-untreated ears, whereas the losses of the OHCs and the IHCs in the treated ears were reduced to 64.0 ± 29.6% and 8.3 ± 3.5%, respectively (Figure 4c). Two-way ANOVA was conducted to examine the effect of the TAT-FNK administration and the type of HC on HC loss. There was no significant interaction between TAT-FNK administration and type of HC ($F_{1,20}=3.055$, $P=0.096$). There were main effects of TAT-FNK administration ($F_{1,20}=6.869$, $P=0.016$) and type of HCs ($F_{1,20}=110.657$, $P<0.01$), indicating that the TAT-FNK treatment significantly attenuated the HC damage induced by KM and EA. Drug control animals administered only TAT-FNK showed minimal HC loss throughout the cochlea.

In vitro effect of TAT-FNK on protection of HCs and caspase-9 activation

Figure 5c shows an intact, untreated cochlear explant that was double-labeled with rhodamine-conjugated phalloidin (red) and activated caspase-9 (green). The stereocilia bundles on the three rows of OHCs and one row of IHCs have normal morphology and negligible green staining. Figure 5a shows a cochlear explant treated with KM for 10 h. HCs are missing and caspase-9 labeling is present in the HC regions. These results indicate that KM treatment caused an increase in caspase-9 activation, leading to apoptosis of the HCs by a mitochondria-mediated pathway. Addition of TAT-FNK to the explants greatly suppressed caspase-9 activation (Figure 5b). The number of HCs with activated caspase-9 in the explants treated only with KM was 20.6 ± 5.2 per 0.2-mm length, whereas the number was reduced to 7.6 ± 3.2 per 0.2-mm length in the explants treated with KM and TAT-FNK (Figure 5d, $n=4$ each). The number of HCs with activated caspase-9 in explants treated with KM and FNK (without TAT) was 16.7 ± 3.2. There was a statistically significant difference between the groups as determined by one-way ANOVA ($F_{3,12}=31.337$, $P<0.01$). Scheffe's *post hoc* test revealed that there were significant differences between the KM with TAT-FNK-treated explants, and the KM-treated explants or the KM with FNK-treated explants ($P<0.01$). There was no statistically significant difference between the KM-treated explants and the KM with FNK-treated explants

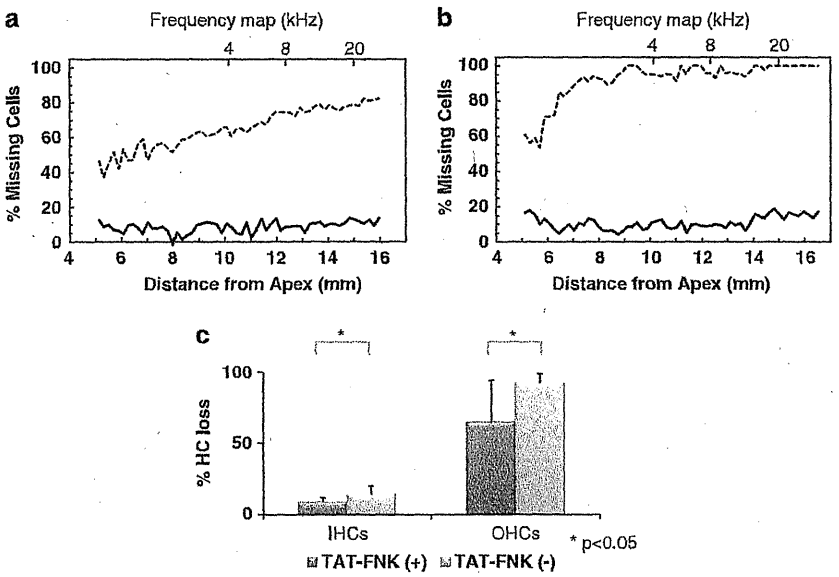

Figure 4. Average cytocochleograms and average missing HCs for each experimental group 2 weeks after exposure to EA and KM. TAT-FNK-untreated ear (**a**). TAT-FNK-treated ear (**b**). The solid line represents the percentage of missing IHCs and the dashed line represents the percentages of missing OHCs. (**c**) The mean number of missing IHCs and OHCs from 5 to 16 mm. Error bar: s.d. $^{*}P<0.05$.

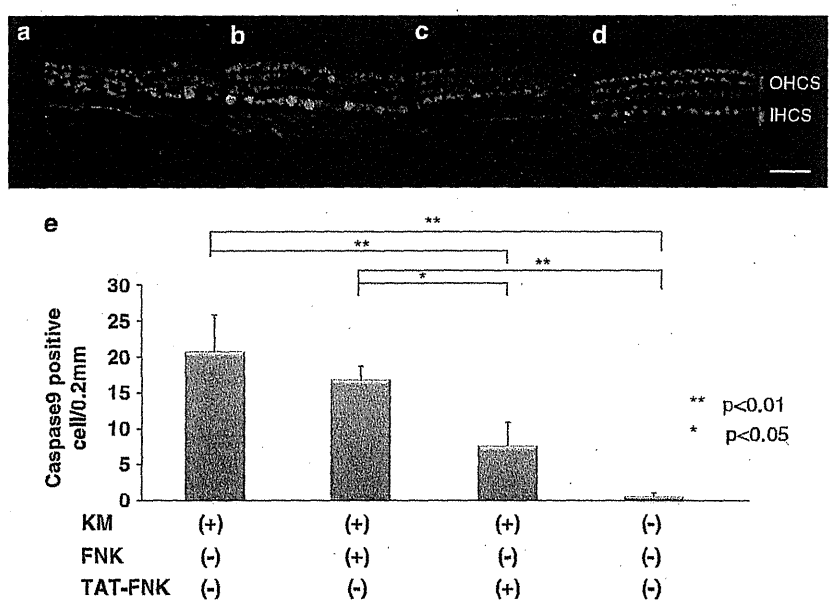

Figure 5. Fluorescence micrographs of caspase-9 activation and HC morphology. Rhodamine phalloidin (red) was used to stain the cell morphology and the fluorescent caspase substrate fam-LEHD-fmk (green) was used to stain caspase-9. Scale bar = 30 μm. (**a**) TAT-FNK-untreated group. (**b**) FNK-treated group. (**c**) TAT-FNK-treated group. (**d**) Control group. (**e**) Mean number of caspase-9-positive HCs (IHCs + OHCs) present in 0.2-mm length of the cochlea. Error bar: s.d. $^{**}P<0.01$; $^{*}P<0.05$.

($P=0.429$). Therefore, the TAT-FNK treatment significantly reduced the number of HCs entering the caspase-9-dependent apoptotic pathway after KM application.

We counted the number of viable HCs ($n=6$ each) after 12 h of culture. In the control that was not administered any additional agent such as KM, FNK or TAT-FNK, no or only few HCs were lost. When the number of viable HCs ($n=6$ each) was counted after 12 h of culture with KM (that is, in the absence of TAT-FNK), massive losses of the OHCs and the IHCs were induced, as only 25.2 ± 9.1% and 28.5 ± 11.9% of the cells survived, respectively. The TAT-FNK treatment attenuated OHC and IHC damages, as 80.1 ± 14.9% and 74.1 ± 20.6%, respectively, of the cells remained. In the explants treated with KM with FNK, the extent of survival was 27.6 ± 5.9% for the OHCs and 38.3 ± 15.9% for the IHCs. Two-way ANOVA was conducted to examine the effect of the drug administration and the type of HC on HC loss. There was a main effect of drug administration ($F_{3,40}=99.432$, $P<0.01$). There was also a main effect of type of HC ($F_{1,40}=419.899$, $P<0.01$). Finally, there was interaction between drug administration and type of HC ($F_{3,40}=47.846$, $P<0.01$). The simple effects analysis revealed significant differences between the KM with TAT-FNK-treated explants, and the KM-treated explants or the KM with FNK-treated

explants ($P<0.01$), in the OHCs. There was no significant difference between the KM-treated explants and the KM with FNK-treated explants. However, in the IHCs, there were no significant differences between the KM with TAT-FNK-treated explants, and the KM-treated explants or the KM with FNK-treated explants. These results indicate that the TAT-FNK treatment significantly attenuated damage to the OHCs; however, FNK alone did not protect the HCs against KM (Figures 6c and d). Drug control animals administered only TAT-FNK showed minor HC loss.

DISCUSSION

In the present study, we demonstrated that the TAT-fusion technique enabled the macromolecule FNK protein, which was infiltrated into a gelatin sponge and placed on the RWM, to successfully enter the cochlea because it allowed the protein to penetrate through the RWM. TAT-myc-FNK was distributed throughout all turns of the cochlea, but immunoreactivity was not observed in the contralateral ears, suggesting that, when topically applied, the distribution of TAT-FNK may be confined to the applied cochlea.

The LIs of TAT-myc-FNK gradually increased until 6 h, but there were no significant differences in the LIs at 1, 3 and 6 h. Beginning at 12 h, the LIs gradually decreased. At 48 h, the immunoreactivity disappeared. This suggests that TAT-myc-FNK was immediately distributed into the cochlea 1 h after administration onto the RWM and remained in high concentration until 6 h. It gradually decreased beginning at 12 h and disappeared by 48 h. When examining the entire cochlea at 6 h after administration of TAT-myc-FNK, the strongest immunoreactivity was present in the cytoplasm of the supporting cells and the HCs in the OC, followed by the SGCs. Immunoreactivity could also be observed in the SV and SL. This suggests that xTAT-myc-FNK was distributed most prominently in the OC followed by SGCs, and that it also reached the SV and SL at 6 h after administration on the RWM. The duration of FNK expression was much longer compared with when it was administered systemically.[13] A single topical administration of TAT-FNK on the RWM effectively protected cochlear HCs from the combination of KM and EA *in vivo*. These findings imply that, when fused with TAT and soaked in a gelatin sponge macromolecular proteins can be applied on the RWM as an effective and selective therapeutic agent to function in the cochlea. Considering the adverse effects introduced by systemic injection, this technology is feasible as a novel treatment for inner ear disorders. TAT-FNK attenuated KM-induced HC death by suppressing the activation of pro-caspase-9 *in vitro*, suggesting that the antiapoptotic protein FNK has the potential to regulate the mitochondria-related apoptotic pathway in the inner ear.

The RWM is a main gate and barrier for various kinds of substances to enter from the middle ear into the inner ear.[19] The membrane consists of three layers: an outer epithelium facing the middle ear, a core of connective tissue and an inner epithelium facing the inner ear.[20–22,16–18] The structure of the outer epithelium is such that substances can pass from the middle to the inner ear by selective absorption and secretion.[23] The factors influencing permeability through the RWM include the molecular weight and configuration of the protein, its contact time and the concentration of the substances in the middle ear.[23–25] Among these, molecular weight is the most important in determining permeability. Generally, low-molecular-weight compounds, such as antibiotics, corticosteroids and labeled ions, can easily pass through the RWM to enter the inner ear,[26,27] whereas penetration of high-molecular-weight substances, such as proteins and lipids, is limited.[19,27–30] In the current study, myc-FNK, whose molecular weight is about 30 kDa, did not pass through the RWM, suggesting that it is too large to pass through. Many proteins related to apoptosis, such as p53, AKT and super oxide dismutase, have a molecular weight of 30–60 kDa. Thus, when considering the

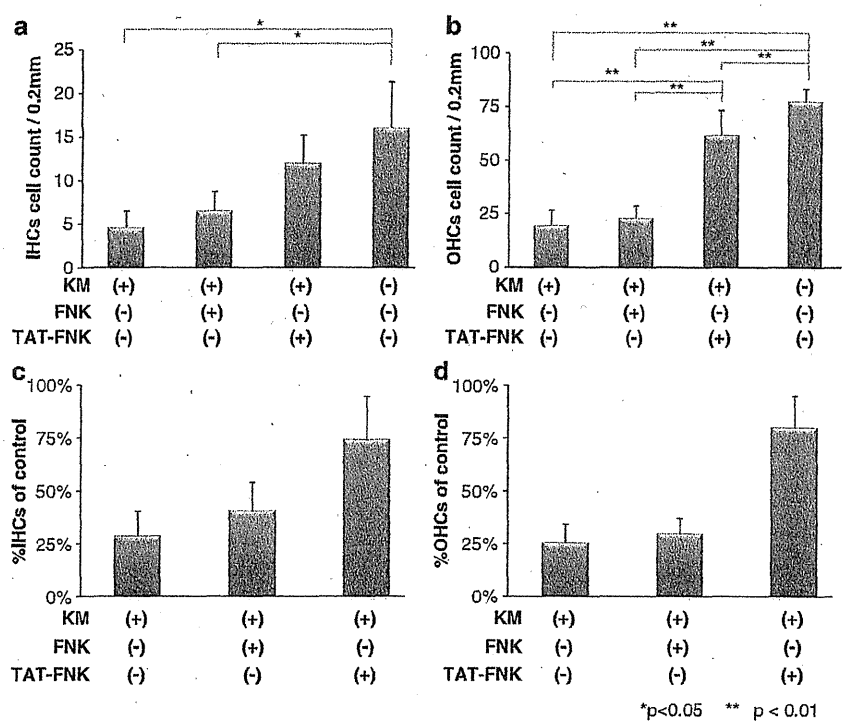

Figure 6. Mean number of surviving HCs of cultured OC after exposure to KM. The mean number of IHCs (**a**) and OHCs (**b**) present in a 0.2-mm length of cochlea taken from four independent parts of the middle cochlear section. Mean percentage of IHCs (**c**) and OHCs (**d**) relative to control cultures. Error bar: s.d. $^{**}P<0.01$; $^{*}P<0.05$.

applicability of protein therapy from the middle ear space, new technology is required to overcome the difficulty of delivering large molecules to the inner ear. The Tat protein of HIV-1 is a protein of 101 residues. The Tat protein has the characteristic that it can cross the plasma membrane of neighboring cells.[31] TAT comprises the short stretches of the Tat protein domain that are primarily responsible for their translocation ability, also referred to as protein transduction domains.[32] Although the exact mechanism has not been elucidated, two models have been proposed: energy-dependent macropinocytosis, and direct uptake by electrostatic interactions and hydrogen bonding.[33] By fusing FNK to the TAT domain, FNK was effectively absorbed into the outer epithelium cells and then secreted to the inner ear space, although further studies are needed to confirm this. When fused with TAT, various proteins were reported to be transported across cell membranes.[7,8] Even β-galactosidase, whose molecular weight is 120 kDa, has been reported to enter cells.[33] Moreover, oligonucleotide, nucleic acids and liposome can also be conjugated with TAT to improve its penetration.[34] Thus, protein transduction technology allows the use of macromolecules for therapeutic application in a variety of inner ear disorders.

In our previous study, we successfully delivered TAT-FNK protein to the inner ear by intraperitoneal injection.[13] However, systemic administration may not be suitable for treatment of inner ear disorders because only relatively small amounts of drug can enter the inner ear, which therefore requires the application of high doses of drug to maintain a therapeutic concentration in the inner ear at an optimal time. Moreover, a single administration has a short half-life, as shown in our previous study,[13] and thus repeated administration is required. High doses of drug may easily induce systemic toxicities and acute allergic side effects. In particular, high doses of this antiapoptotic protein may promote tumor, although this has not been reported. Therefore, injection of drugs topically into the middle ear space may be more appropriate to better control local drug delivery. Injection of drugs into the middle ear space, however, may result in a large portion of the drug being absorbed by the middle ear mucosa or drained into the epipharynx by the Eustachian tube.[35]

To deliver a drug more effectively into the inner ear, using an absorbable material as a drug carrier may be promising. These materials could secure the stability of drugs on the RWM, and thereby lengthen the contact time with the RWM, and reduce diffusion into the mucosa and drainage from the middle ear space.[36] In the current study, we used a gelatin sponge as a carrier of TAT-FNK, as Husmann *et al.*[37] used a gelatin sponge on the RWM to topically apply gentamicin, which then induced severe damage to the cochlea compared with a single application. Similarly, Okamoto *et al.*[38] used a gelatin sponge containing bone morphogenetic protein-2, and demonstrated that bone morphogenetic protein-2 was slowly released and induced successful regeneration of cartilage in a canine tracheomalacia model. Compared with our previous systemic study,[13] we could observe immunoreactivity of TAT-myc-FNK in the cochlea using approximately 1/600th the amount of TAT-myc-FNK. Immunoreactivity of TAT-myc-FNK could still be observed in the cochlea after 24 h, which is significantly longer than the expression periods observed in previous systemic injection studies targeting organs, including the cochlea.[11,13] Further, the amount of TAT-FNK we topically applied to protect HCs from ototoxicity was approximately 1/15th the dose we used systemically to protect from the same ototoxicity in our previous study.[13] Thus, a gelatin sponge is considered to be an effective drug carrier for inner ear disorders.

When drugs are topically applied onto the RWM, they diffuse from the basal end of the cochlea and thus initially show a concentration gradient, decreasing toward the apex. The concentration gradient in the perilymph was investigated, and the greater concentration was demonstrated at the basal turn.[39,40] However, when the patterns of distribution of the drugs applied on the RWM were investigated by immunocytochemistry, the drugs appeared to be widely and rapidly distributed into the various organs of the inner ear. Imamura and Adams[40] examined the distribution of gentamicin in the inner ear of guinea pig using a monoclonal antibody. When gentamicin was placed on the RWM, the entire cochlear cell was diffusely stained until 6 h after administration. Beginning at 6 h after application, staining was found to be localized mainly in the basal turn. Greater staining in the basal turn was also found when gentamicin was administered systemically. These results suggest that gentamicin can be diffused rapidly into the entire cochlea, and that the localization of staining in the basal turn is due to the nature of the cells in the basal turn to accumulate the drug, and not because of the predominant distribution of gentamicin at the basal turn. Zou *et al.*[42] examined the distribution of lipid nanocapsules in cochlear cells after application on the RWM by using fluorescein isothiocyanate and rhodamine-B labeling. The lipid nanocapsules were present in the SGCs, OC and SV 30 min after application. Moreover, the nanocapsules were more strongly distributed in the SV in the second turn than in the basal turn. They assumed that after penetrating the RWM, the nanocapsules are rapidly diffused through the porous modiolar wall of the scala tympani, after which they enter the SGCs, and then are widely diffused through its nerve fibers. In the present study, although there was a trend of higher intensity of immunoreactivity of TAT-myc-FNK at the basal turn, we did not observe statistically significant differences among the turns. We assume that this rapid and relatively even distribution of TAT-FNK throughout the cochlea was achieved by this radial diffusion through the modiolus, and not by longitudinal perilymph diffusion. Pathways to uptake lipid nanocapsules and TAT-mediated particles into the tissue might be similar, as their high permeability is considered to accelerate their rapid diffusion.[41,42] High immunoreactivity in the SGCs compared with those in the SV and SL at 6 h can support this argument, although the cause of the higher immunoreactivity in the OC compared with that in the SGCs needs to be clarified in future research.

It is known that high-frequency hearing loss occurs initially after AG ototoxicity. However, when the damage by AG is severe, apical cells will be affected and hearing loss expands to lower frequencies.[43] The doses of the KM and EA combination we chose were assumed to be sufficient to cause threshold shifts even at a low frequency. We observed some tendency that the OHCs in the basal parts are more susceptible to the combination of EA and KM than those the upper parts (Figures 4a and b). This finding is consistent with that in other studies.[44] When we compared the extent of missing HCs in the region corresponding to the frequency at which ABR was measured, the percentages of missing OHCs was approximately 67% in the region corresponding approximately to 4 kHz and 80% in that corresponding to 20 kHz. In untreated ears, the percentages of missing OHCs in the regions comparable to 4 and 20 kHz were 95% and 100%, respectively. The differences in the extent of OHC loss between the 4- and 20-kHz regions were small, supporting the ABR findings that there was no significant difference in the threshold shifts among the tested frequencies, although the ABR threshold shifts were slightly greater at higher frequencies than at lower frequencies.

In the current study, we showed that caspase-9 was activated by KM *in vitro*. This finding suggests that KM-induced cochlear HC death is caspase-9-dependent, which is consistent with other studies.[1,45] We demonstrated that TAT-FNK suppressed the activation of caspase-9 in this study and reduced the extent of cleaved PARP in OHCs in our previous study,[13] which suggests that TAT-FNK prevents the intrinsic apoptotic pathway, as does the parent protein Bcl-x_L. It has also been shown that TAT-FNK affects the cytosolic movement of Ca^{2+} and protects neuronal cells from glutamate excitotoxicity.[11] It has been shown *in vitro* that AG antibiotics cause an increase in intracellular calcium levels

in avian HCs[46] and in isolated OHCs of guinea pigs.[47] Therefore, inhibition of Ca^{2+} homeostasis distribution may have a crucial role in the ability of TAT-FNK to prevent apoptotic cochlear HC death. The mechanism of how TAT-FNK prevents cochlear HC death remains to be fully elucidated.

In conclusion, we demonstrated that TAT-FNK infiltrated in gelatin sponge and placed on the guinea pig RWM could successfully deliver the protein to the cochlea by penetrating through the RWM, and that a single topical administration of TAT-FNK protected the cochlea against the combination of the ototoxic drugs KM and EA *in vivo*. An *in vitro* study demonstrated that TAT-FNK suppressed the activation of caspase-9 and protected cochlear HCs from KM-induced apoptosis. These findings suggest that topical administration of an antiapoptotic protein fused with TAT and soaked with a gelatin sponge is effective at preventing the apoptosis of cochlear HCs, and that such topical treatment is superior to systemic administration in terms of organ specificity and safety. Future studies using this technology may extend the feasibility of protein therapy for treatment of inner ear disorders.

MATERIALS AND METHODS

The experimental protocol was approved by the University Committee for the Use and Care of Animals at the University of Tokyo, and it conforms to the NIH Guidelines for the Care and Use of Laboratory Animals.

Construction and preparation of TAT-FNK and TAT-myc-FNK

We constructed FNK (originally designated as Bcl-xFNK) by introducing amino-acid substitutions into Bcl-x_L using a two-step PCR mutagenesis method, as reported previously.[9] The substituted codons were as follows: Tyr-22 (TAC) with Phe (TTC), Gln-26 (CAG) with Asn (AAC) and Arg-165 (CGG) with Lys (AAG). Among the mammalian antiapoptotic factors, FNK is the only mutant with a gain-of-function phenotype because, compared with Bcl-x_L, FNK showed stronger antiapoptotic activity to protect cultured cells from death induced by various death stimuli, including oxidative stress, a calcium ionophore and withdrawal of growth factors.[9] TAT-FNK and TAT-myc-FNK were then prepared as described previously.[11] The gene constructed for FNK was fused with an oligonucleotide encoding TAT, and the resulting TAT-FNK gene encoded met-gly-TAT (consisting of 11 amino acids: YGRKKRRQRRR)-gly-FNK. An oligonucleotide encoding GEQKLISEEDLG (the myc TAG sequence is underlined) was inserted between the TAT and FNK sequences of TAT-FNK by PCR to obtain TAT-myc-FNK. To construct myc-FNK without the TAT domain, an oligonucleotide encoding met-gly-myc TAG-gly was also ligated to the FNK sequence by PCR. The TAT-FNK plasmid was introduced into *Escherichia coli* DH5a cells (Invitrogen, Life Technology, Carlsbad, CA, USA) and the TAT-FNK protein was overexpressed by treatment with 1 mM isopropyl 1-thio-β-D-galactoside for 5 h with vigorous shaking at 37 °C. Proteins were solubilized in buffer (7 M urea, 2% sodium dodecyl sulfate, 1 mM dithiothreitol, 62.5 mM Tris-HCl (pH 6.8) and 150 mM NaCl) and then subjected to sodium dodecyl sulfate-PAGE to remove contaminating proteins and endotoxins. The gel was treated with 1 M KCl and the transparent band corresponding to TAT-FNK was cut out. Proteins were electrophoretically extracted from the gel slice using extraction buffer (25 mM Tris, 0.2 M glycine and 0.1% sodium dodecyl sulfate) for *in vitro* and *in vivo* experiments. The extraction buffer was used as the vehicle. The concentration of the extracted TAT-FNK ranged from 1 to 6 mg ml^{-1}.

Immunohistochemical detection of TAT-myc-FNK in the cochlea after tympanic administration

Eighteen male albino guinea pigs (Saitama Experimental Animals Supply Co. Ltd, Saitama, Japan) weighing 250–300 *g* were used. Under anesthesia with xylazine hydrochloride (10 mg kg^{-1}; Bayer, Leverkusen, Germany) and ketamine hydrochloride (40 mg kg^{-1}; Sankyo, Tokyo, Japan), a postauricular incision was made and the bone posterior to the tympanic ring was exposed. A hole was drilled into the bulla exposing the middle ear space medial to the tympanic ring. The round window niche and the RWM were identified. The gelatin sponge (Spongel; Astellas Pharma Inc., Tokyo, Japan) was soaked in 3 μl of TAT-myc-FNK (0.5 mg ml^{-1}) and placed on the RWM of the left ear. The animals were killed at 1, 3, 6, 12, 24 and 48 h ($n = 3$ for each time point) after injection, while under deep anesthesia, using an overdose of xylazine hydrochloride (Bayer) and ketamine hydrochloride (Sankyo). Three animals that were killed 6 h after a similar tympanic administration of myc-FNK (3 μl; 0.5 mg ml^{-1}) served as controls. The cochleae from both ears were perfused with 4% paraformaldehyde in 0.1 M phosphate-buffered saline (PBS) at pH 7.4 through the oval and round windows, and immersed in the same fixative overnight at 4 °C. The specimens were decalcified in 10% EDTA acid for 14 days, dehydrated through a graded alcohol series and embedded in paraffin. The embedded tissues were cut into 5-μm-thick sections parallel to the modiolus and mounted on glass slides. The sections were deparaffinized, hydrated and rinsed with PBS. To detect TAT-myc-FNK and myc-FNK *in situ*, rabbit an anti-myc-tag polyclonal antibody was used (1:5000, 4 °C overnight; Upstate Biotechnology, Lake Placid, NY, USA) coupled with a DAKO Envision + system (Dako Japan, Kyoto, Japan). Negative controls were established by replacing the primary antibody with blocking buffer.

The LI of the anti-myc antibody in the cochlear tissues was obtained by a modified Photoshop-based image analysis. The original method was developed by Lehr *et al*.[48] In brief, an image was digitized on magnetic optical disks. Using the 'Magic Wand' tool in the 'Select' menu of Photoshop, the cursor was placed on a portion of the immunostained area. The tolerance level of the Magic Wand tool was adjusted so that the entire immunostained area was selected. Using the 'Similar' command in the 'Select' menu, all the immunostained areas were selected automatically. Subsequently, the image was transformed to an 8-bit grayscale format. An optical density plot of the selected areas was generated using the 'Histogram' tool in the 'Image' menu. The mean staining intensity and the number of pixels in the selected areas were quantified. Next, the background was selected using the 'Inverse' tool in the 'Select' menu. The mean background intensity was quantified using the 'Histogram' tool as mentioned above. The immunostaining intensity was calculated as the difference between the mean staining intensity and the mean background intensity. The immunostained ratio was calculated as the ratio of the number of pixels in all the immunostained areas to that in the entire image. LI was defined as the product of the immunostained ratio and the immunostaining intensity. The modiolar sections were obtained in every third section and five sections were randomly selected from each ear (10 sections from each animal). As a result, the LI was measured using 30 sections in each group by a technician naïve to the treatment, preparation techniques or the aims of the current study. To investigate differences among the cochlear turns, the LIs in the basal, second and third turns were also measured 1 and 6 h after application. The LIs of the SGCs, SV and SL 6 h after the application of TAT-myc-FNK onto the RWM, as well as those in the controls, were also measured. To compare the immunostaining intensity among the cells in these organs, the ratios of normalized immunoreactivity were calculated by dividing the LIs at 6 h by those of the control.

Tympanic injection of TAT-FNK *in vivo*

Eight male albino guinea pigs, weighing 250–300 g and showing ABR thresholds within normal limits based on our laboratory database, were used in this investigation. Only male animals were used because there are gender differences in the ability to detoxify reactive oxygen species and in the levels of endogenous antioxidants in the cochlea.[49,50]

Animals were anesthetized with xylazine hydrochloride (10 mg kg^{-1}) and ketamine hydrochloride (40 mg kg^{-1}). Chloramphenicol sodium succinate (30 mg kg^{-1}, intramuscular injection) was administered as a prophylactic. Under aseptic conditions, the bulla was exposed bilaterally from an occipitolateral approach and opened to allow visualization of the RWM. A gelatin sponge soaked with 3 μl of TAT-FNK (6 mg ml^{-1}) was placed on the RWM in the left ear, whereas a gelatin sponge soaked with only a vehicle was placed on the RWM in the right ear. One hour after the wound was sutured, a single dose of KM (200 mg kg^{-1}; Meiji, Tokyo, Japan)

was injected subcutaneously. Then, 2 h after the KM injection, the jugular vein was exposed under general anesthesia and EA (40 mg kg^{-1}; Sigma-Aldrich, Tokyo, Japan) was infused into the vein as described previously.[51] An additional four animals served as drug controls: a gelatin sponge soaked with 3 µl of TAT-FNK (6 mg ml^{-1}) was placed on the left RWM, but KM and EA were not administered.

ABR measurement

ABRs were recorded using waveform storing and stimulus control using MEB-5504 (NIHON KOHODEN CO., Tokyo Japan) and DPS-725 (DIA MEDICAL CO., Tokyo, Japan). Sound stimuli were produced by the PT-R7 III ribbon-type speaker (PIONEER CO., Tokyo, Japan). Recordings were performed in a closed-field TRAACOUSTICS acoustic enclosure (TRACOUSTICS INC., Austin, TX, USA) and sound level calibration was performed using a sound-level meter (NA-28 RION, Tokyo, Japan). Pure tones (4, 8 and 20 kHz) were measured 3 days after the arrival of the animals to determine the baseline thresholds, and 14 days after the ototoxic insult (for experimental animals) or TAT-FNK application (for drug control animals) to determine the threshold shifts. The frequencies (4, 8 and 20 kHz) measured in this study were frequently used for other studies using guinea pigs, including our previous study.[13,52,53] We have limited our investigation to these frequencies to evaluate hearing to minimize the stress on these animals. The method of ABR measurement has been described previously.[54] In brief, animals were anesthetized with a mixture of xylazine hydrochloride (10 mg kg^{-1}, intramuscular) and ketamine hydrochloride (40 mg kg^{-1}, intramuscular), and needle electrodes were placed subcutaneously at the vertex (active electrode), beneath the pinna of the measured ear (reference electrode) and beneath the opposite ear (ground). The stimulus duration was 15 ms, with a presentation rate of 11 s^{-1}, and the rise/fall time was 1 ms. Responses of 1024 sweeps were averaged at each intensity level (5-dB steps) to assess the threshold. The threshold was defined as the lowest intensity level at which a clear reproducible waveform was visible in the trace. When an ABR waveform could not be evoked, the threshold was assumed to be 5 dB greater than the maximum intensity produced by the system (105 dB SPL). Threshold shifts were calculated by subtracting the baseline thresholds from those observed before killing.

Assessment of extent of HC loss

After ABR measurements 14 days after ototoxic insults (experimental animals) or TAT-FNK application (drug control animals), animals were killed under deep anesthesia using xylazine hydrochloride and ketamine hydrochloride. The bilateral cochleae were perfused with 4% paraformaldehyde in 0.1 M PBS at pH 7.4 through the oval and round windows, and then immersed in the same fixative overnight at 4 °C. The cochleae were then washed with PBS, permeabilized with 0.3% Triton X-100 for 10 min and labeled with 1% rhodamine phalloidin (Molecular Probes, Eugene, OR, USA) for 30 min to stain F-actin. The tissues were processed as whole mounts using the surface preparation technique. The specimens were then mounted on glass slides using the Prolong Antifade kit (Molecular Probes) and observed. Reticules whose length (bin width) at × 40 was 0.45 mm were used to count the numbers of total and missing HCs. HCs that showed an identifiable cell body and cuticular plate were considered to be present. The presence of distinctive scar formations produced by convergence of adjacent phalangeal processes was regarded as an indicator of a missing HC. The percentage of HC loss for the IHCs and OHCs was calculated for each segment obtained from each animal. The average for each segment was then determined for each group and plotted from the apex to the base to produce an average cytocochleogram. Two animals were excluded because of tissue damage during surface preparation, leaving a total of six cochleae for the HC count study.

Assessment of the protective effects of TAT-FNK and caspase-9 detection for cultured HCs

Sprague–Dawley rats (Saitama Experimental Animals Supply Co. Ltd) were decapitated on postnatal day 5 (P5) and the cochlea was carefully dissected out. On the basis of the methods of Sobkowicz *et al.*,[55] the SV, the SL and the spiral ganglion neurons were dissected away, leaving the OC. The cochlea used for analysis was prepared by cutting 2 mm from the basal end and 3 mm from the apical end of the cochlea (approximately half of the cochlea). Explants were maintained in Dulbecco's modified Eagle's medium with 10% fetal bovine serum, 25 mM Hepes and 30 U ml^{-1} penicillin, and were cultured in an incubator at 37 °C under 5% CO_2 and 95% humidity for 24 h. Explants were exposed to medium containing 20 nM TAT-FNK, 20 nM FNK without TAT or vehicle. Two hours after exposure, the medium was changed to one containing 6 mM KM and either 20 nM FNK, 20 nM TAT-FNK or the vehicle. Typically, 10 cultures were evaluated for each experimental condition: four were cultured for 10 h for detection of caspase-9 and six were cultured for 12 h for cell counting. Additional 10 cultures were evaluated for control, of which four were cultured for 10 h and six were cultured for 12 h, with the medium containing no KM.

Caspase-9 activity was examined by using the fluorescent caspase substrate fam-LEHD-fmk (caspase-9 substrate), which was obtained from Intergen (Purchase, NY, USA) and used according to the manufacturer's protocol. After culturing, the fluorescent substrate was added directly to the culture medium (final concentration, 5 µM) for the final hour in culture. After 1 h in this substrate, the OC was washed three times for 15 min each at 37 °C in the washing buffer supplied by the manufacturer. The cultures were then fixed overnight at 4 °C in the fixative supplied by the manufacturer. After fixation, the cochleae were washed with PBS, permeabilized with 0.3% Triton X-100 for 10 min and labeled with 1% rhodamine phalloidin (Molecular Probes) for 30 min to stain F-actin. Whole mounted cochleae were viewed with a confocal laser-scanning microscope (ZEISS LSM5 PASCAL). Caspase-9-positive cells were counted over a 0.2 mm longitudinal distance from four separate regions in each culture. A mean value was determined for each culture.

For HC counting, cultures were fixed overnight at 4 °C in the fixative supplied by the manufacturer. After fixation, the cochleae were washed with PBS, permeabilized with 0.3% Triton X-100 for 10 min and labeled with 1% rhodamine phalloidin (Molecular Probes) for 30 min to stain F-actin. To quantify HC loss in the cochlea after various treatments, IHCs and OHCs were counted over a 0.2 mm longitudinal distance from four separate regions of each culture. A mean value was determined for each culture.

Statistical analysis

The SPSS software was used for statistical analysis. The time course of the LI for TAT-myc-FNK in the OC was compared between groups by one-way and then pairwise comparisons, with statistical significance adjusted for multiple comparisons (Scheffe's test). The differences in the turns of the LI for TAT-myc-FNK in the OC at 1 and 6 h were compared by two-way ANOVA (the independent variables were cochlear turns and time course). The differences in the normalized LIs between the sub-sites in the cochlea were compared by one-way ANOVA, and then pairwise comparisons were performed by using Scheffe's test. The ABR thresholds at each frequency before and 14 days after the ototoxic insults were compared by two-way ANOVA (the independent variables were TAT-FNK administration and hearing frequency). The extent of missing HCs *in vitro* was also compared by two-way ANOVA (the independent variables were TAT-FNK treatment and type of HC). Caspase-9 activities between the groups were compared by one-way ANOVA followed by Scheffe's test. The extent of missing HCs *in vitro* after exposure to KM was compared by two-way ANOVA (the independent variables were type of HC and drug administration), and if a statistically significant interaction was observed, Bonferroni test was used for simple effects analysis. A level of $P<0.05$ was accepted as statistically significant.

CONFLICT OF INTEREST

The authors declare no conflict of interest.

ACKNOWLEDGEMENTS

We thank Ms A Tsuyuzaki and Ms Y Kurasawa (Department of Otolaryngology and Head and Neck Surgery, Faculty of Medicine, University of Tokyo, Tokyo, Japan) for technical assistance. This work was supported by Grants (17659527 and 20390440)

from the Ministry of Education, Culture, Sports, Science, and Technology of Japan to TY and a Grant (15110201) from the Ministry of Health, Labor and Welfare of Japan to TY.

REFERENCES

1 Cheng AG, Cunningham LL, Rubel EW. Mechanisms of hair cell death and protection. *Curr Opin Otolaryngol Head Neck Surg* 2005; **13**: 343–348.
2 Rybak LP, Whitworth CA, Mukherjea D, Ramkumar V. Mechanisms of cisplatin-induced ototoxicity and prevention. *Hear Res* 2007; **226**: 157–167.
3 Rizzi MD, Hirose K. Aminoglycoside ototoxicity. *Curr Opin Otolaryngol Head Neck Surg* 2007; **15**: 352–357.
4 Staecker H, Liu W, Malgrange B, Lefebvre PP, Van De Water TR. Vector-mediated delivery of bcl-2 prevents degeneration of auditory hair cells and neurons after injury. *ORL J Otorhinolaryngol Relat Spec* 2007; **69**: 43–50.
5 Liu YH, Ke XM, Qin Y, Gu ZP, Xiao SF. Adeno-associated virus-mediated Bcl-xL prevents aminoglycoside-induced hearing loss in mice. *Chin Med J* 2007; **120**: 1236–1240.
6 Haas R, Murea S. The role of granulocyte colony-stimulating factor in mobilization and transplantation of peripheral blood progenitor and stem cells. *Cytokines Mol Ther* 1995; **1**: 249–270.
7 Schwarze SR, Ho A, Vocero-Akbani A, Dowdy SF. *In vivo* protein transduction: delivery of a biologically active protein into the mouse. *Science* 1999; **285**: 1569–1572.
8 Becker-Hapak M, McAllister SS, Dowdy SF. TAT-mediated protein transduction into mammalian cells. *Methods* 2001; **24**: 247–256.
9 Asoh S, Ohtsu T, Ohta S. The super antiapoptotic factor Bcl-xFNK constructed by disturbing intramolecular polar interactions in rat Bcl-xL. *J Biol Chem* 2000; **275**: 37240–37245.
10 Asoh S, Mori T, Nagai S, Yamagata K, Nishimaki K, Miyato Y *et al.* Zonal necrosis prevented by transduction of the artificial anti-death FNK protein. *Cell Death Differ* 2005; **12**: 384–394.
11 Asoh S, Ohsawa I, Mori T, Katsura K, Hiraide T, Katayama Y *et al.* Protection against ischemic brain injury by protein therapeutics. *Proc Natl Acad Sci USA* 2002; **99**: 17107–17112.
12 Nagai S, Asoh S, Kobayashi Y, Shidara Y, Mori T, Suzuki M *et al.* Protection of hepatic cells from apoptosis induced by ischemia/reperfusion injury by protein therapeutics. *Hepatol Res* 2007; **37**: 133–142.
13 Kashio A, Sakamoto T, Suzukawa K, Asoh S, Ohta S, Yamasoba T. A protein derived from the fusion of TAT peptide and FNK, a Bcl-x(L) derivative, prevents cochlear hair cell death from aminoglycoside ototoxicity *in vivo*. *J Neurosci Res* 2007; **85**: 1403–1412.
14 Minn AJ, Boise LH, Thompson CB. Expression of Bcl-xL and loss of p53 can cooperate to overcome a cell cycle checkpoint induced by mitotic spindle damage. *Genes Dev* 1996; **10**: 2621–2631.
15 Valera ET, Brassesco MS, Scrideli CA, Tone LG. Tetraploidization in Wilms tumor in an infant. *Genet Mol Res* 2010; **9**: 1577–1581.
16 Schuknecht HF. Ablation therapy for the relief of Meniere's disease. *Trans Am Laryngol Rhinol Otol Soc* 1956; **66**: 589–600.
17 Haynes DS, O'Malley M, Cohen S, Watford K, Labadie RF. Intratympanic dexamethasone for sudden sensorineural hearing loss after failure of systemic therapy. *Laryngoscope* 2007; **117**: 3–15.
18 Tsuji J, Liberman MC. Intracellular labeling of auditory nerve fibers in guinea pig: central and peripheral projections. *J Comp Neurol* 1997; **381**: 188–202.
19 Tanaka K, Motomura S. Permeability of the labyrinthine windows in guinea pigs. *Arch Otorhinolaryngol* 1981; **233**: 67–73.
20 Bellucci RJ, Fisher EG, Rhodin J. Ultrastructure of the round window membrane. *Laryngoscope* 1972; **82**: 1021–1026.
21 Carpenter AM, Muchow D, Goycoolea MV. Ultrastructural studies of the human round window membrane. *Arch Otolaryngol Head Neck Surg* 1989; **115**: 585–590.
22 Miriszlai E, Benedeczky I, Horváth K, Köllner P. Ultrastructural organization of the round window membrane in the infant human middle ear. *ORL J Otorhinolaryngol Relat Spec* 1983; **45**: 29–38.
23 Goycoolea MV, Lundman L. Round window membrane. Structure function and permeability: a review. *Microsc Res Tech* 1997; **36**: 201–211.
24 Lundman LA, Holmquist L, Bagger-Sjoback D. Round window membrane permeability. An *in vitro* model. *Acta Otolaryngol* 1987; **104**: 472–480.
25 Juhn SK, Hamaguchi Y, Goycoolea M. Review of round window membrane permeability. *Acta Otolaryngol Suppl* 1989; **457**: 43–48.
26 Smith BM, Myers MG. The penetration of gentamicin and neomycin into perilymph across the round window membrane. *Otolaryngol Head Neck Surg* 1979; **87**: 888–891.
27 Brady DR, Pearce JP, Juhn SK. Permeability of round window membrane to 22Na or RISA. *Arch Otorhinolaryngol* 1976; **214**: 183–184.
28 Nomura Y. Otological significance of the round window. *Adv Otorhinolaryngol* 1984; **33**: 1–162.
29 Morizono T, Hamaguchi Y, Juhn SK. *Permeability of human serum albumin from chinchilla middle ear to inner ear. In XXIII workshop on inner ear biology 1986*. GDR: Berlin.
30 Goycoolea MV, Paparella MM, Goldberg B, Carpenter AM. Permeability of the round window membrane in otitis media. *Arch Otolaryngol* 1980; **106**: 430–433.
31 Richard JP, Melikov K, Vives E, Ramos C, Verbeure B, Gait MJ *et al.* Cell-penetrating peptides. A reevaluation of the mechanism of cellular uptake. *J Biol Chem* 2003; **278**: 585–590.
32 Vivès E, Brodin P, Lebleu B. A truncated HIV-1 Tat protein basic domain rapidly translocates through the plasma membrane and accumulates in the cell nucleus. *J Biol Chem* 1997; **272**: 16010–16017.
33 Wadia JS, Dowdy SF. Protein transduction technology. *Curr Opin Biotechnol* 2002; **13**: 52–56.
34 Gupta B, Levchenko TS, Torchilin VP. Intracellular delivery of large molecules and small particles by cell-penetrating proteins and peptides. *Adv Drug Deliv Rev* 2005; **57**: 637–651.
35 Ruel-Gariepy E, Chenite A, Chaput C, Guirguis S, Leroux J. Characterization of thermosensitive chitosan gels for the sustained delivery of drugs. *Int J Pharm* 2000; **203**: 89–98.
36 Park AH, Jackson A, Hunter L, McGill L, Simonsen SE, Alder SC *et al.* Cross-linked hydrogels for middle ear packing. *Otol Neurotol* 2006; **27**: 1170–1175.
37 Husmann KR, Morgan AS, Girod DA, Durham D. Round window administration of gentamicin: a new method for the study of ototoxicity of cochlear hair cells. *Hear Res* 1998; **125**: 109–119.
38 Okamoto T, Yamamoto Y, Gotoh M, Huang CL, Nakamura T, Shimizu Y *et al.* Slow release of bone morphogenetic protein 2 from a gelatin sponge to promote regeneration of tracheal cartilage in a canine model. *J Thorac Cardiovasc Surg* 2004; **127**: 329–334.
39 Salt AN. Simulation of methods for drug delivery to the cochlear fluids. *Adv Otorhinolaryngol* 2002; **59**: 140–148.
40 Imamura S, Adams JC. Distribution of gentamicin in the guinea pig inner ear after local or systemic application. *J Assoc Res Otolaryngol* 2003; **4**: 176–195.
41 Zou J, Saulnier P, Perrier T, Zhang Y, Manninen T, Toppila E *et al.* Distribution of lipid nanocapsules in different cochlear cell populations after round window membrane permeation. *J Biomed Mater Res B Appl Biomater* 2008; **87**: 10–18.
42 Khalil IA, Kogure K, Akita H, Harashima H. Uptake pathways and subsequent intracellular trafficking in nonviral gene delivery. *Pharmacol Rev* 2006; **58**: 32–45.
43 Chen Y, Huang WG, Zha DJ, Qiu JH, Wang JL, Sha SH, Schacht J. Aspirin attenuates gentamicin ototoxicity: from the laboratory to the clinic. *Hear Res* 2007; **226**: 178–182.
44 Priuska EM, Schacht J. Mechanism and prevention of aminoglycoside ototoxicity: outer hair cells as targets and tools. *J Ear Nose Throat J* 1997; **76**: 164–166, 168, 170–1.
45 Cunningham LL, Cheng AG, Rubel EW. Caspase activation in hair cells of the mouse utricle exposed to neomycin. *J Neurosci* 2002; **22**: 8532–8540.
46 Hirose K, Westrum LE, Stone JS, Zirpel L, Rubel EW. Dynamic studies of ototoxicity in mature avian auditory epithelium. *Ann NY Acad Sci* 1999; **884**: 389–409.
47 Li Y, Huang Y, Luo S. Alternation of intracellular Ca2+ caused by streptomycin in the isolated cochlear OHC. *Zhonghua Er Bi Yan Hou Ke Za Zhi* 1995; **30**: 227–229.
48 Lehr HA, Mankoff DA, Corwin D, Santeusanio G, Gown AM. Application of Photoshop-based image analysis to quantification of hormone receptor expression in breast cancer. *J Histochem Cytochem* 1997; **45**: 1559–1565.
49 Julicher RH, Sterrenberg L, Haenen GR, Bast A, Noordhoek J. Sex differences in the cellular defence system against free radicals from oxygen or drug metabolites in rat. *Arch Toxicol* 1984; **56**: 83–86.
50 el Barbary A, Altschuler RA, Schacht J. Glutathione S-transferases in the organ of Corti of the rat: enzymatic activity, subunit composition and immunohistochemical localization. *Hear Res* 1993; **71**: 80–90.
51 Yamasoba T, Kondo K. Supporting cell proliferation after hair cell injury in mature guinea pig cochlea *in vivo*. *Cell Tissue Res* 2006; **325**: 23–31.
52 Suzuki M, Yagi M, Brown JN, Miller AL, Miller JM, Raphael Y. Effect of transgenic GDNF expression on gentamicin-induced cochlear and vestibular toxicity. *Gene Ther* 2000; **7**: 1046–1054.
53 Lin CD, Oshima T, Oda K, Yamauchi D, Tsai MH, Kobayashi T. Ototoxic interaction of kanamycin and 3-nitropropionic acid. *Acta Otolaryngol* 2008; **128**: 1280–1285.
54 Pourbakht A, Yamasoba T. Ebselen attenuates cochlear damage caused by acoustic trauma. *Hear Res* 2003; **181**: 100–108.
55 Sobkowicz HM, Loftus JM, Slapnick SM. Tissue culture of the organ of Corti. *Acta Otolaryngol Suppl* 1993; **502**: 3–36.

Chapter 14
Frontiers in the Treatment of Hearing Loss

Tatsuya Yamasoba, Josef M. Miller, Mats Ulfendahl, and Richard A. Altschuler

1 Introduction

In the last decade, a paradigm shift has occurred in our vision for the prevention and treatment of hearing impairment. No longer are the solutions restricted to hearing aids, surgery, and implants to restore hearing, control of serum levels to prevent drug-induced ototoxicity, hearing protectors to prevent noise-induced hearing loss (NIHL), and for hereditary loss: wait and hope. Obviously all but the latter practices are of vital continued value, but the promise of more varied and more effective opportunities to prevent hearing loss and to restore hearing have provided increased hope and opportunity. Our future vision is now filled with complex pharmaceutical, cellular, and molecular strategies to modulate hereditary loss, replace and regenerate tissues of the inner ear, and prevent drug-induced hearing loss and NIHL. This future holds the promise of dramatically reducing the lost educational and job opportunities, the social isolation, and the reduced quality of life that accompanies hearing impairment and deafness, and with it the enormous economic costs associated with health care and lost productivity (estimated by the World Health Organization at >2% world GNP). This future molds and reshapes the practices of audiology and otolaryngology to place far greater efforts on the prevention of hearing impairment and the use of local and systemic drug treatment to restore hearing.

A new vision for treatment is based on an increased understanding of the cellular and molecular mechanisms underlying the progression of pathology from an initiating event to hearing impairment. Figure 14.1 diagrams this progression and

J.M. Miller (✉)
Department of Otolaryngology and Department of Cell & Developmental Biology
Kresge Hearing Research Institute, 1150 West Medical Center Drive,
Ann Arbor, MI 48109-5616, USA
e-mail: josef@umich.edu

C.G. Le Prell et al. (eds.), *Noise-Induced Hearing Loss: Scientific Advances*,
Springer Handbook of Auditory Research 40, DOI 10.1007/978-1-4419-9523-0_14,

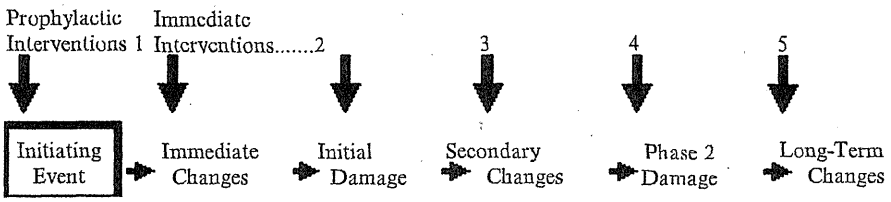

Fig. 14.1 A schematic of the events in the progression of pathology from an initiating event such as noise overstimulation to the long-term changes associated with hearing impairment. Arrows mark the opportunities for interventions for prevention, repair, and rescue, ranging from prophylactic interventions before the initiating event, and immediate interventions after the event, to treatments after damage has progressed

indicates multiple potential timings for interventions. The initiating event could be intense noise, an ototoxic drug, a viral agent, an autoimmune response, or any other traumatic event.

This initiating event leads to immediate changes, which could be common to most traumatic events or could be restricted to a specific trauma such as noise. Resulting changes could be in metabolic activity, reactive oxygen species (ROS) formation, blood flow, stress response, or excitotoxicity, all of which occur after noise (for detailed reviews, see Hu, Chap. 4; Le Prell & Bao, Chap. 13). Some of these could result in immediate initial damage, for example, excitotoxicity resulting in bursting of auditory nerve peripheral processes. Prophylactic or immediate post-trauma interventions could target these immediate changes and prevent the initial damage. In the absence of immediate intervention, there is a subsequent progression of secondary changes. These can induce and influence intracellular pathways, such as those leading toward cell death or protection, and can also set in motion cellular and molecular changes both in the cochlea and in central auditory pathways (see, e.g., Kaltenbach, Chap. 8, for detailed discussion of central auditory system plasticity post-noise). Thus, both the cochlea and the central auditory system provide targets for interventions. The progression of these secondary insult pathways can lead to apoptotic cell death and additional waves of cell damage progressing over hours, days, and weeks, with targets for interventions diminishing over time as events proceed. Once the damage is complete, the long-term changes remain, including hearing loss or hearing disorders, and the need for treatments for cure or improvement.

Many of the cellular and molecular mechanisms associated with the different pathologies and changes along this progression, as well as interventions and methods of accomplishing interventions, are considered in more detail in the other chapters. Here we relate these new insights in mechanisms to the potential clinical interventions that may treat the inner ear to prevent hearing loss or restore lost hearing. The most optimal intervention and intervention time may not always be practical when brought into a real-life situation, and alternative approaches must be considered. Translational studies based on basic research, identification of mechanisms, and potential interventions (sites and times) will have a feed-forward influence on validating (or not) our understanding and interpretation of mechanisms underlying